Shallow groundwater level time series and a groundwater chemistry survey from a boreal headwater catchment, Krycklan, Sweden

Jana Erdbrügger[1], Ilja van Meerveld[1], Jan Seibert[1, 2], Kevin Bishop[2]

[1]Department of Geography, University of Zurich, Zurich, Switzerland
[2]Department of Aquatic Sciences and Assessment, Swedish University of Agricultural Sciences, Uppsala, Sweden

Correspondence to: Jana Erdbrügger (jana.erdbruegger@geo.uzh.ch)

Abstract. Shallow groundwater can respond quickly to precipitation and is the main contributor to streamflow in most catchments in humid, temperate climates. Therefore, it is important to have high spatial and temporal resolution data on groundwater levels and groundwater chemistry to test spatially distributed hydrological models. However, currently, there are few datasets on groundwater levels with a high spatial and temporal resolution because of the large effort required to collect these data. To better understand shallow groundwater dynamics in a boreal headwater catchment, we installed a network of groundwater wells in two areas in the Krycklan catchment in Northern Sweden: a small headwater catchment (3.5 ha, 54 wells) and a hillslope (1 ha, 21 wells). The average well depth was 274 cm (range: 70 - 581 cm). We recorded the groundwater level variation at a 10-30 min interval between 18. July 2018 – 1. November 2020. Manual water level measurements (0 - 26 per well) during the summers of 2018 and 2019 were used to confirm and re-calibrate the automatic water level measurements. The groundwater level data for each well was carefully processed using six data quality labels. The absolute and relative positions of the wells were measured with a high-precision GPS and terrestrial laser scanner (TLS) to determine differences in absolute groundwater levels and calculate groundwater gradients. During the summer of 2019, all wells with sufficient water were sampled once and analyzed for electrical conductivity, pH, absorbance, anion and cation concentrations, as well as the stable isotopes of hydrogen and oxygen. The data are available at https://doi.org/10.5880/fidgeo.2022.020 (Erdbrügger et al., 2022). This combined hydrometric and hydrochemical dataset can be useful for testing models that simulate groundwater dynamics and evaluating metrics that describe subsurface hydrological connectivity.

1. Introduction

In most headwater catchments in temperate climates, streamflow during rainfall or snowmelt events is dominated by shallow groundwater flow from unconfined aquifers in the soil or regolith, or groundwater perched above a less permeable layer. Shallow groundwater levels can increase quickly during rainfall or snowmelt events, and can vary considerably over distances of just several meters (van Meerveld et

al., 2015; Moore and Thompson, 1996; Myrabø, 1997; Seibert et al., 2003; Tromp-van Meerveld and McDonnell, 2006).

Shallow groundwater is essential for streamflow and stream chemistry in headwater catchments. In many boreal ecosystems, shallow groundwater is also a major source of solutes to streamflow, such as nitrogen (Sponseller et al., 2016), dissolved organic carbon (Buffam et al., 2011; Ploum et al., 2020), or mercury (e.g., Eklöf et al., 2015; Munthe and Hultberg, 2004; Vidon, 2012). An accurate simulation of flow pathways and solute transport requires a good understanding of the groundwater flow directions, which depends on the difference in absolute groundwater levels. In temperate climates, shallow groundwater levels are assumed to be related to topography (Condon and Maxwell, 2015; Haitjema and Mitchell-Bruker, 2005; Tóth, 1962; Winter, 1999), but flow directions can change significantly over time and space. They tend to be more slope-parallel during wet periods with high groundwater levels and more stream-parallel during drier periods (e.g., Rodhe and Seibert, 2011; van Meerveld et al., 2015). The direction can even change from being directed towards the stream to away from the stream (Covino and McGlynn, 2007; Doering et al., 2007; Payn et al., 2009; Simpson and Meixner, 2013; Ward et al., 2013; Yu et al., 2013; Zimmer and McGlynn, 2017). Thus, spatial and temporal resolution measurements of groundwater levels can help to improve our understanding of hydrological systems and their functioning. High-resolution groundwater data are also useful to better understand the relation between the depth to groundwater and vegetation (e.g., Bachmair et al., 2012), to test hydrological models (e.g., Jutebring Sterte, 2016) or methods to simulate groundwater levels at unmonitored sites or derived variables. For example, several approaches have been used to quantify hydrological connectivity based on groundwater level data and topography. Rinderer et al. (2019) estimated groundwater levels for unmonitored sites based on the relation between relative groundwater levels and the topographic wetness index (TWI; Beven and Kirkby, 1979), and Jencso et al. (2009) estimated the duration of hillslope stream connectivity based on the upslope accumulated area. However, due to the lack of high-resolution groundwater level data in both space and time, these approaches have rarely been tested for multiple catchments.

Groundwater level data are often collected by regulatory or environmental management agencies, such as Sveriges Geologiska Undersökning (SGU) in Sweden. Although these datasets include observations for many groundwater wells, they mainly contain data on groundwater levels in major aquifers, reflecting the direct societal importance of these aquifers as a water resource. These datasets generally have no or only minimal data for shallow unconfined aquifers in headwater catchments. Furthermore, the spacing of the wells is usually too wide to allow for the calculation of the groundwater flow directions (but see Fan (2019) and Fan and Schaller (2009), who used data from these types of datasets to determine the vertical component of groundwater flow across the US).

Groundwater level data have been collected at a high spatial and temporal resolution for a few research catchments (see Table A 1 for an overview). For example, Jencso et al. (2009) continuously measured groundwater levels in 84 wells across the 17.2 km^2 Tenderfoot Creek Experimental Forest in Montana,

USA, and Rinderer et al. (2014) did so for 51 wells in the 20 ha Studibach catchment in Switzerland. A few other studies took manual measurements at many wells (e.g., Moore and Thompson, 1996; Myrabø, 1997), or combined manual measurements with data loggers (e.g., Bonanno et al. 2021). Other studies have collected high spatial resolution groundwater data for individual hillslopes (for examples see Table A 1).

One reason so few high-spatial and temporal resolution groundwater level datasets exist is the high cost (both time and money) to install and maintain a dense groundwater monitoring network (see also Retike et al., 2022). Until a few decades ago, water level sensors with an integrated logger or options for wireless data transmission were not readily available. This implied that automatic measurements in multiple groundwater wells required either multiple data loggers, which were rather expensive, or that sensors were connected to a single data logger by wires, which limited the maximum distance between them or caused other problems (e.g., broken cables and an increased the risk of damage by lightning). Sensors and data loggers were also more expensive then. Where multiple wells had been drilled in a catchment, the groundwater level measurements were mainly often done by hand, resulting in low temporal resolution data (e.g., Bishop et al., 2011; Seibert et al., 2011; see also Table A1).

In addition to recent advances in data logging, there have also been advances in the development of handheld (but powered) augers (e.g., Gabrielli and Mcdonnell, 2012), which makes it easier to install multiple wells in a reasonable amount of time. Drilling rigs and drilling services have become more readily available as well. This has made drilling in remote terrain more practical and installing a dense well network easier, though it is still costly and time-consuming (see section 4.2). However, to calculate flow directions, the elevation of the wells and their position also need to be known accurately (Rau et al., 2019). While this can be done with traditional surveying methods, terrestrial LiDAR measurements have made it easier to determine the exact position of groundwater wells in the landscape. In summary, recent technological advances in data logging, drilling, and surveying, have made it easier to collect high-resolution groundwater-level data. However, there are still very few public datasets with high temporal and spatial resolution groundwater data due to the time and effort needed to collect, clean and publish the data (Retike et al., 2022).

Here, we present a unique dataset with two years of groundwater level data for 54 wells in a 3.5 ha headwater catchment and 20 wells in a 1 ha study area within the Krycklan catchment in Northern Sweden. Streamflow in this catchment is dominated by shallow groundwater flow (Laudon et al., 2013, 2021). The shallow aquifer in the study catchment consists primarily of till that is relatively uniform in its lateral extent. Long-term data for precipitation and streamflow make the two years of groundwater measurements even more helpful for model testing purposes. In addition to the groundwater level data, we also present the results of a sampling campaign during the summer of 2019 to determine the spatial variability in groundwater chemistry. Shallow groundwater chemistry can be highly spatially variable across headwater catchments (e.g., Kiewiet et al., 2019; Penna and van Meerveld, 2019). Groundwater chemistry data help study groundwater flow pathways and validate hydrological or nutrient-transport

models (e.g., Kolbe et al., 2020). In this manuscript, we describe the groundwater level and chemistry
110   data (see also Table A 2 for a brief description of the two datasets, the files for each dataset, and the
information contained in each file).

2.   Description of the Study Areas

The Krycklan research catchment (6790 ha) is located in Northern Sweden, about 60 km inland from
115   Umeå (64°140N, 19°460E; Figure 1). The region has a cold temperate humid climate, with on average
167 days of persistent snow cover (1981–2020 period), but this duration has been declining in recent
years (Laudon et al., 2021). The mean annual temperature (1981–2010) is 1.8° C; with a mean
temperature in January of -9.5 °C and a mean temperature of 14.7 °C in July). The mean annual
precipitation is 614 mm/y and the mean annual runoff is 311 mm/y (Laudon et al., 2013, 2021).
120   The hilly landscape consists of rock outcrops, pine (Pinus sylvestris) and spruce (Picea abies) forest
(87%), and mires (9%). The landscape is strongly influenced by the last glaciation 10,000 years ago,
which left glacial tills up to ten meters deep overlying the metamorphic bedrock. The highest postglacial
coastline crosses the study area at an elevation of approximately 257 m above mean sea level (amsl).
The soils that developed in the till are podzols, except at the base of the slopes where organogenic soils
125   have developed. The soil is thin close to the rock outcrops near the ridges and up to 10 m towards the
streams. The saturated hydraulic conductivity of the soil declines rapidly with depth below the surface
(at least for the upper meter of the soil (Bishop et al., 1990)). The shallow aquifers in the till are relatively
uniform in lateral extent. The groundwater tables are generally shallow (< 6 m from the surface and in
most locations < 2 m). Shallow groundwater flow is the main source of streamflow (Ledesma et al.,
130   2018; Lyon et al., 2012) and is driven by the topography (Leach et al., 2017; Ploum et al., 2020). About
15 m to 20 m below the water table, the water age increases by several decades (Kolbe et al., 2020).
More information on the soils, geomorphology, geology, and hydrology of the Krycklan catchment can
be found in Laudon et al., (2013), Ivarsson and Johnson (1988) and Ivarsson (2007).

The wells described in this manuscript are located in two study areas in the core area of the Krycklan
135   research catchment (Figure 1). One area is located in what is called sub-catchment 6 (110 ha) in other
studies (e.g., Laudon et al., 2021). This is referred to as study area A here. The other area is located near
what is called the S-transect in sub-catchment 2 (12 ha). This area is, hereafter, referred to as area B.
The elevation of the study areas ranges from approximately 250-270 m amsl. Both study areas are
located within the zone that has been protected since 1922. Forestry activities have been limited in these
140   areas, but the areas were subject to ditching at the beginning of the 1900s (Laudon et al., 2013, 2021).
A particular advantage of obtaining high spatial and temporal resolution groundwater data in the
Krycklan catchment is the abundance of other hydrometric data (e.g., precipitation, streamflow since
1981), vegetation, and soil data (Laudon et al., 2021, 2013). This includes atmospheric data since 2011
from the Integrated Carbon Observatory System (ICOS) Svartberget station (ICOS, 2021), which is

145 located close (<500 m) from the study areas. Long-term soil and groundwater chemistry data are available for 16 groundwater wells (2 m - 12 m) since 1989 (4 wells) and 2012 (16 wells) (Laudon et al., 2013).
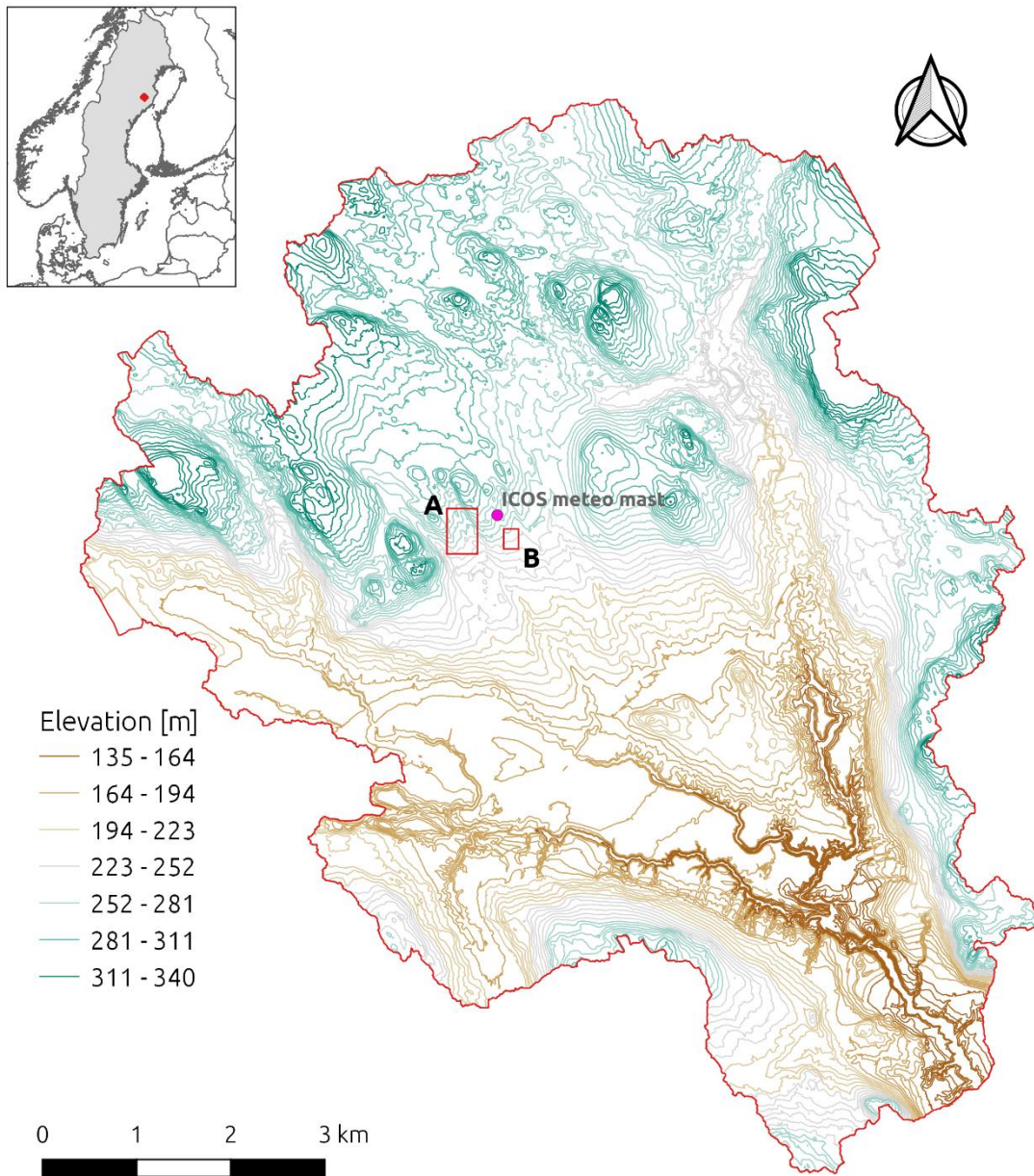
Figure 1: The Krycklan catchment and the location of the two study areas where the groundwater wells were installed
150 **(red squares, A (in C6) and B (S-transect in C2)). The location of the ICOS station is marked by a point (north of area B). The inset shows the location in of the Krycklan catchment in Northern Sweden. See Figure 2 for a more detailed map of the study areas. Datum: Swerref99 TM, EPSG 3006.**

3. Groundwater wells

3.1 Well network design

155 The locations for the wells were chosen based on the LiDAR-derived digital elevation model (DEM), with a closer well spacing in areas where we either expected very stable or very variable flow directions/gradients (Erdbrügger et al., 2021). To allow determining groundwater gradients (i.e., flow

directions), the wells were located in triangles of different sizes: 5 m, 10 m and 20 m (Figure 2). In the field, the planned positions of the wells were identified with a handheld GPS, and the help of elevation and vegetation maps. Not all wells could be installed as planned. For some locations, the position had to be adjusted due to the presence of trees and big boulders. In addition, the access requirements for the drill rig (see section 3.2) meant that the location of some of the wells had to be moved. However, in most cases, the wells could be installed within 5 m of the pre-determined positions based on the DEM.
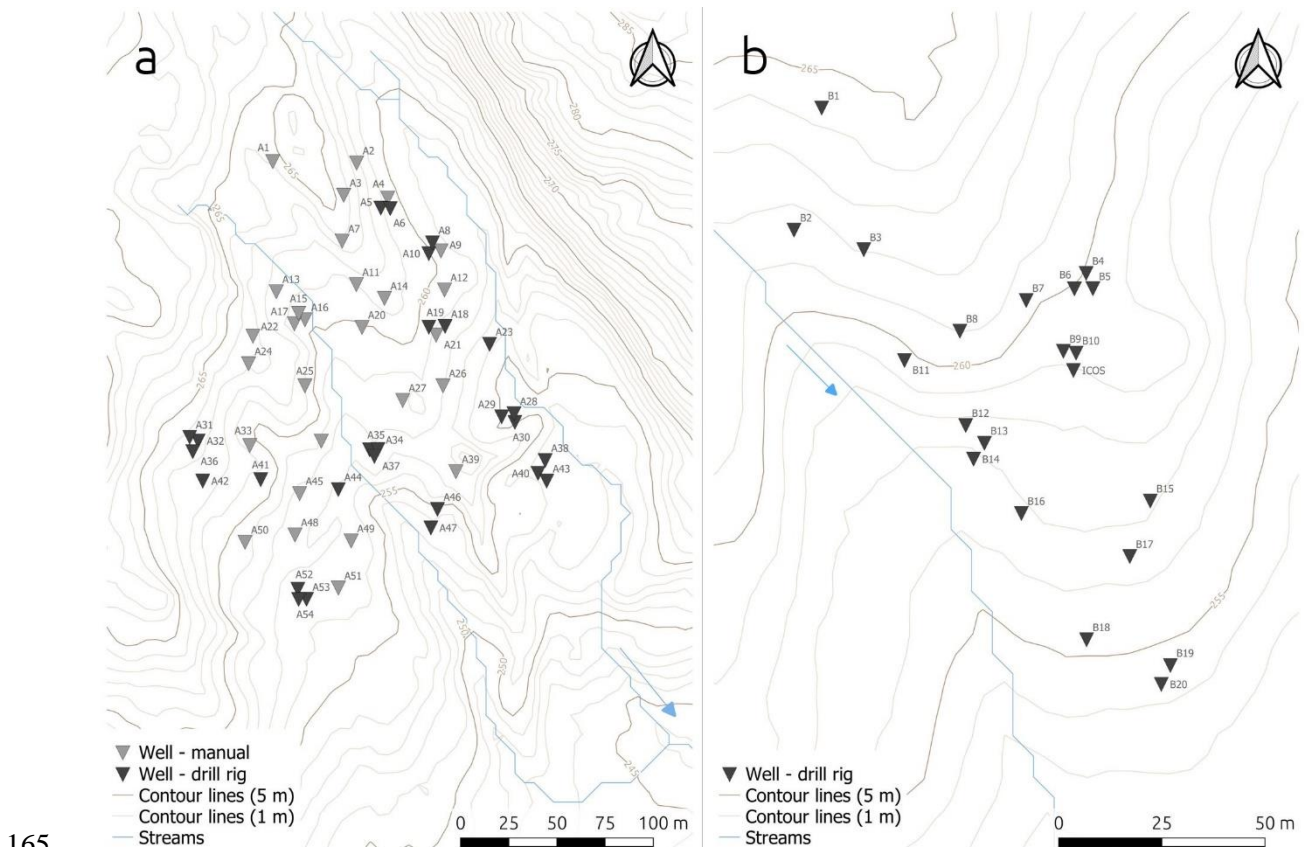
Figure 2: Maps of the two study areas (A (a) and B (b)) with the location of the 75 wells (triangles) that were either augured by hand (manual, in light gray) or installed by the drill rig (dark gray). The letters next to each triangle indicate the name of the well. See Figure 1 for the location of the two study areas within the Krycklan catchment.

3.2 Well installation

We installed 27 wells with a Cobra™ Petrol-Driven Drill and Breaker between May and October 2018 (all in area A) and 48 wells (27 in area A and 21 in area B) with a drill rig between February and March 2019 (Figure 2 and Figure 3). The drill rig was used in winter, when the ground was frozen and covered by a thick snowpack, to minimize the impact of the heavy machinery on soil and vegetation. The wells consist of fully screened PVC pipes with an outer diameter of 5.0 cm and an inner diameter of 3.7 cm. A filter sock was placed over the entire screened length of the pipe to limit the entry of particles into the well.

The required well depths were estimated based on the "Depth to Water" index (Murphy et al., 2009) which was calculated based on the DEM but was adjusted based on the groundwater levels observed

180   during installation. Many of the wells needed to be deeper than suggested by the index. For the installations during winter, the required depths were based on the groundwater depths measured in the summer. We tried to install the wells at least one meter deeper than the lowest observed groundwater level in nearby wells. The target depth could not be reached in some cases due to boulders or other obstacles. As a result, some wells were not sufficiently deep to measure the groundwater level during

185   the driest periods. This was particularly the case for the wells located furthest away from surface water bodies. The average depth of the wells was 274 cm (standard deviation: 113 cm; range: 57 - 578 cm). The depth of the wells installed in summer (with Cobra) was generally less (average 193 cm; range: 57 cm – 386 cm) than for the wells installed in winter with the drill rig (average: 316 cm; range 168 cm – 578 cm).

190   The height of the top of the wells above the ground (i.e., the stick-up) was measured after installation, on three occasions in 2018 and two occasions in 2019. A marker on the pipe ensured that this height was always measured on the same side of the pipe. The position of the well tops may have shifted slightly over the measurement period due to freezing and thawing of the ground. Soil heave in the Krycklan catchment can be several centimeters over the frost season (Bergsten et al., 2001). We,

195   however, assume that this effect was minor for the wells (and thus the well tops) because the pipes reached well below the average freeze/thaw line, which is located at -19 cm in the Krycklan catchment (Panneer Selvam et al., 2016). Thus, although the relation of the tube top to the soil surface may have changed slightly over time due to soil heave, as well as trampling, we assume that the relation of the well tops to each other remained the same.

200

Table 1: Estimated costs for installing the well network

What	Notes	Cost
Well installation with machinery	February-March 2019, drilling company in charge of 52 wells with depths ranging from 2 – 5 m (including installation of fully screened PVC pipes)	~15 500 EUR (~300 EUR per well)
Well installation manually	Summer season 2018, 3 student interns for 3 months (half-time) with Cobra	~ 5 800 EUR for a new cobra, plus payment of staff
PVC pipe and filter sock	Fully screened PVC groundwater tubes, filter sock, etc.	~10-20 EUR per well
Water level loggers	Depending on cable length. In total 75 wells equipped Odyssey capacitance water level loggers (Dataflow Systems Ltd, 2021)	~ 210 EUR per logger
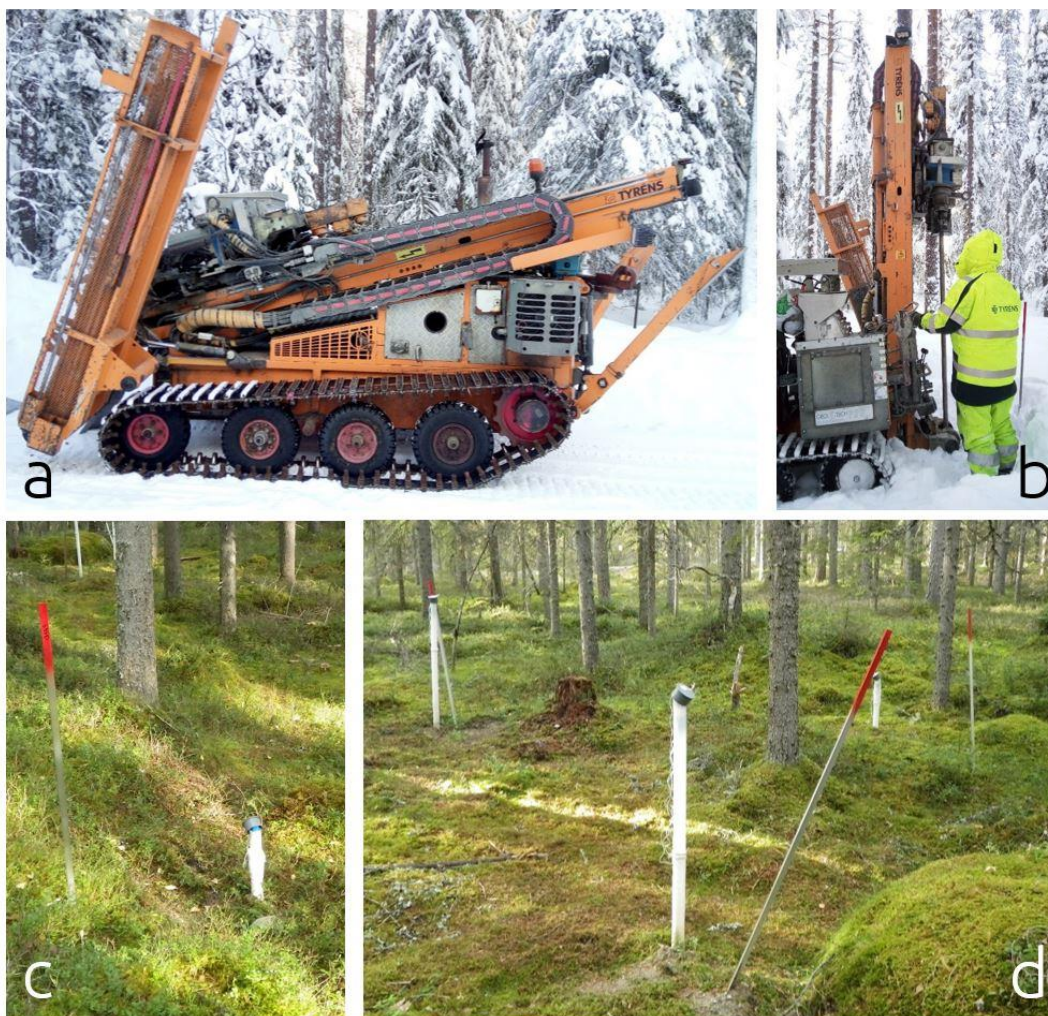
Figure 3: (a) and (b) Well installation in winter 2019, and (c) and (d) pictures of closely positioned wells that form triangles (length of pipe above ground ~ 50 cm in panel (c) and 110 cm in panel (d)). The gray caps were placed over the loggers for protection. The aluminum poles with the red paint next to the wells were used to determine the location of the wells when snow covered the ground.

3.3 Well geo-referencing

After installation, the position of the wells was determined with a high-precision GPS. All wells were scanned with a terrestrial laser scanner (Trimble TX8) in May 2019 to more accurately determine their vertical and horizontal position relative to each other. About 68 single scans (39 in area A and 29 in area B) were done at a distance of about 20 m. The scan resolution at 30 m from the scanner was one point every 11.3 mm (Drive and Trimble Inc., 2017). The generated point clouds were combined into one large point cloud following the procedure proposed by the Ljungberget Remote Sensing Laboratory at the Swedish University of Agricultural Sciences (Bohlin and Nyström, 2019). The wells were manually identified in the combined point cloud, and the upper end of the tube was taken as the reference point (Figure 4). The relative positions of the wells are given in the Krycklan_gw_wells.csv file. The registration reports are given in the 2022-020_Erdbruegger-et-al_TLS_registration_area[A/B].rtf files; the complete scan data are available via the Krycklan database (Lindgren, 2021).

The positions of the well tops were exported as an ESRI shape-file. We then used a similarity transformation (only rotations and x and y offsets, no scaling) to georeference the well positions (x and y coordinates only). As orientation points for the similarity transformation, we used the locations of four wells measured in the field with the high-precision GPS. Since the scan was already level in the horizontal direction (using the TLS internal leveling), we adjusted the z-offset by the GPS z-position of one of the wells to obtain a general offset for all wells. The procedure was carried out separately for the two study areas (A, B) (Table 3).
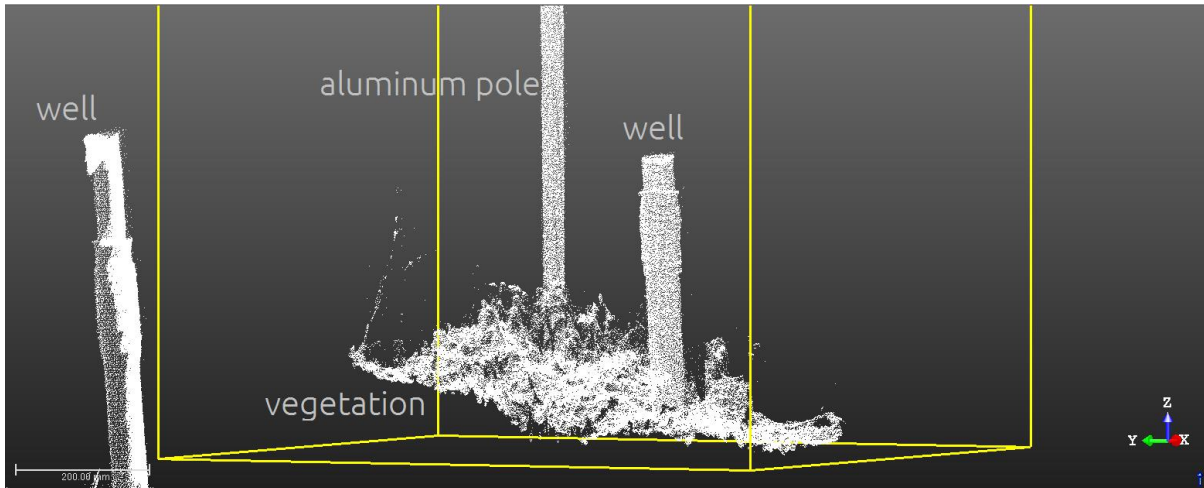
Figure 4: Example of the point clouds for manually identified wells. The well (on the right and in the foreground on the left), filter sock, and the aluminum pole (in the middle, top cut off) marking the well and surrounding vegetation are clearly visible in the point cloud.

4. Dataset 1: Groundwater levels

4.1 Dataset structure

The groundwater level dataset (Dataset 1) consists of two files. One file (2022-020_Erdbruegger-et-al_Krycklan_gw_wells.csv) provides a description of each well and the other file (2022-020_Erdbruegger-et-al_Krycklan_gw_wells.csv) provides the time series of the actual measurements and the calculated water level in meters above mean sea level (m amsl) for each well. See Table A 3: Structure of the groundwater well location data file (2022-020_Erdbruegger-et-al_Krycklan_gw_wells.csv) and description of the column names and Table A 4: Structure of the groundwater level data file (2022-020_Erdbruegger-et-al_Krycklan_gw_levels.csv) and description of the column names for the structure of these datafiles, respectively. The measurements and data processing steps to obtain the time series of the groundwater levels are described in the following sections.

4.2 Manual water level measurements

The distance between the top of the well and the water level (*man_level*) was manually measured weekly to bi-weekly in July, September and October 2018 and between May and September 2019. On average, the depth to the water level could be manually measured 14 times (range: 0-26). For shallow (< 1 m) groundwater levels, we usually used a bubbler to measure the distance between the top of the well and the water level. When the water level was deeper, we used either a water level plopper ("kluk lod" in Swedish) or an acoustic water level sounder because the bubbler did not work as well for these conditions. For more detailed information on these manual measurements, see Appendix A.

The distance to the water level was noted directly in a spreadsheet and on paper for cross-referencing after the fieldwork. These data were screened visually and checked for plausibility. Data points that deviated strongly from the expected range were double-checked based on field notes, meteorological data, and data from nearby wells. Data entries outside the expected range that could not be confirmed by any other source were classified as outliers. In total, five manual measurements that deviated more than 1 m from the expected value were excluded and are assumed to have been entered incorrectly in the datasheets.

4.3 Continuous water level measurements

4.3.1 Initial logger calibration, installation and maintenance

For the continuous water level measurements, we installed capacitance water level loggers (Dataflow Systems PTY Limited, Christchurch, New Zealand) in 74 wells. The length of the cable of the water level loggers was based on the depth of the well and the expected changes in water level. Although we used loggers with different housing lengths and cable lengths, they all function similarly (see Appendix A). The resolution of the sensors is 0.8 mm (Dataflow Systems Ltd, 2021).

All loggers were calibrated according to the instructions provided by the supplier (Dataflow Systems PTY Limited, 2012) prior to field installation. In short, two points (at 20 cm and 140 cm from the lower end of the weight at the end of the cable; see Figure A 1) were marked and the logger was suspended in a sealed PVC pipe filled with water from one of the groundwater wells so that the water reached exactly the mark on the cable. For each position, the raw measurement values were noted after an acclimatization phase of about half a minute or until the values had stabilized. This two-point linear calibration was used to convert the raw sensor values to distances (in cm) above the bottom of the sensor.

The loggers were set to record at a 10 min interval, except in the first measurement week when it was 15 min, and in winter 2018/2019 when it was set to 30 min to avoid filling the memory (and overwriting the data) during the winter period. The data were downloaded three or four times during the field season (May to October). Loggers that did not record any data or only recorded data for part of the period were inspected and usually reinstalled the same day or the following day.

We had to take the loggers out of the wells for the manual water level measurements. We tried to time this so that it would not coincide with the measurements (i.e., we aimed to do this within the 10 min

interval between measurements). When the data were being downloaded, the loggers were inspected visually for any disturbances, such as biofilm or dirt on the cable, kinks, or obstructions, and were
285   cleaned when necessary. At this time, we also measured and adjusted the logger string lengths if the groundwater level had fallen, or was expected to fall, below the deepest point of the sensor, or if it was expected to rise above the logger body during snowmelt.

The groundwater level (*Log_level_uncorr*) in cm below the top of the well was calculated by subtracting the water level measured by the logger (in cm from the bottom of the logger weight) from the sum of
290   the length of the logger body, cable and weight length, and string length (see Figure A 1). These water level time series were inspected manually for incongruences. For five wells, the string length information was accidentally not recorded for all periods (after adjustments due to very high or very low water levels in the well), so the groundwater level below the top of the well could not be calculated; these data points were marked (*Offset* flag, see section 4.4), and can only be used to investigate
295   groundwater level dynamics but not the actual level.

4.3.2   Logger level data correction (re-calibration)

When analyzing the data, it became apparent that there was a systematic offset between the logger data (*Log_level_uncorr*) and the manual measurements (*man_level*) (Figure 5 (a) and (c)), with the logger-based water levels being systematically higher (i.e., closer to the surface) than the manual measurements.
300   In some cases, they were above the surface, although we only observed flooding for two of the wells (i.e., only for these two wells did we expect the water levels to rise above the ground surface at some point in the year). We deemed the manual measurements more reliable and assumed that the shift was due to a systematic error in the initial calibration of the loggers or calculation of the logged water levels. We can exclude pipe length (which would have been an individual error for each well) and string length
305   (the shift also appears for loggers that were not attached to strings) as the source of the systematic error and, therefore, assume that the shift was due to a systematic offset in the calibration of the loggers before field deployment.

We corrected the logger data in a two-step process based on the assumption that we only needed to correct the vertical shift in the logger data. We first determined the linear regression between the manual
310   measurements and logger data, using a slope of one. We then defined points more than 5 cm from this initial linear regression as outliers caused by errors in the manual water level measurements. After excluding these outliers, we determined a new linear regression between the manual measurements and logger-derived water level data, again with a slope of one, and calculated the offset (see two examples of the correction in Figure 5). The mean value for this correction (i.e., *intercept*) was -9.91 cm (standard
315   deviation: 6.74 cm; range: -28.1 - -0.05 cm). We then used this offset (*intercept*) to correct the logger data. Thus, effectively, we lowered the logger data to match the manual water level measurements. This fixed the issues with the water levels rising above the surface for all wells for which this was not

observed. The data were not corrected for 18 of the 74 wells because there were less than two valid manual water level measurements to calculate the correction (i.e., *intercept*).

320   The final absolute groundwater level (*Log_level_corr*; in m asl) was calculated by adding the correction factor (*intercept*) to the uncorrected logger level (*log_level_uncor*) and the elevation of the well top (*Z_abs*): *Log_level_corr = Z_abs – (Log_level_uncorr+intercept)*.
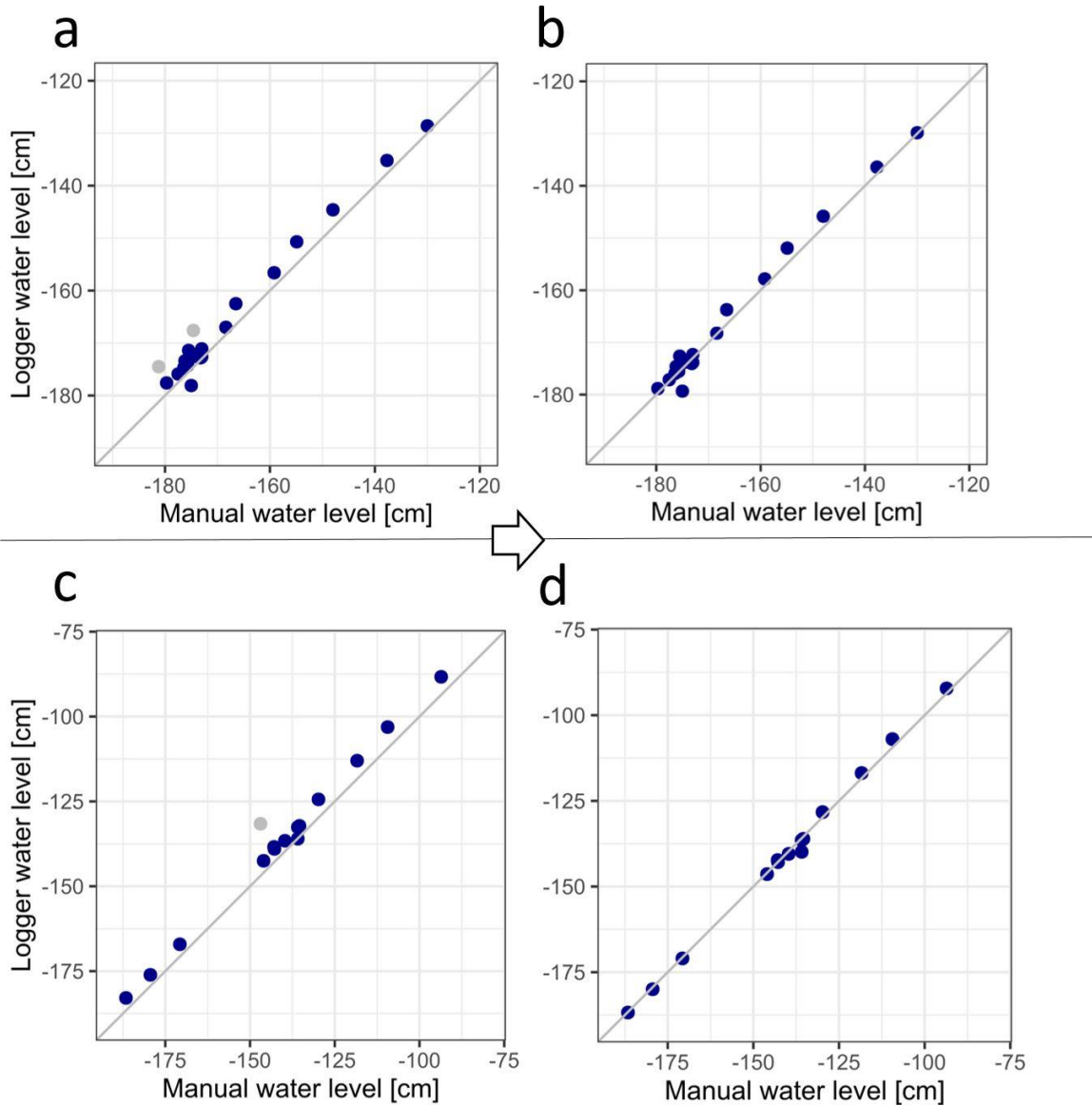
325   **Figure 5: Relation between the manual and logger water level measurements in cm below the top of the well before ((a) and (c)) and after ((b) and (d)) recalibration of the logger for well A7 ((a) and (b)) and well B18 ((c) and (d)). Manual measurements which were identified as outliers are marked in gray (in (a) and (c)). The correction factor (i.e., intercept) was -1.2 cm for well A7 and - 3.9 cm for well B18.**

4.4 Data Flagging

Outliers or discontinuities in the water level time series were classified into six different categories (Table A 5; Figure 6). This flagging allowed us to keep all data points in the record so that they could be re-evaluated if necessary.
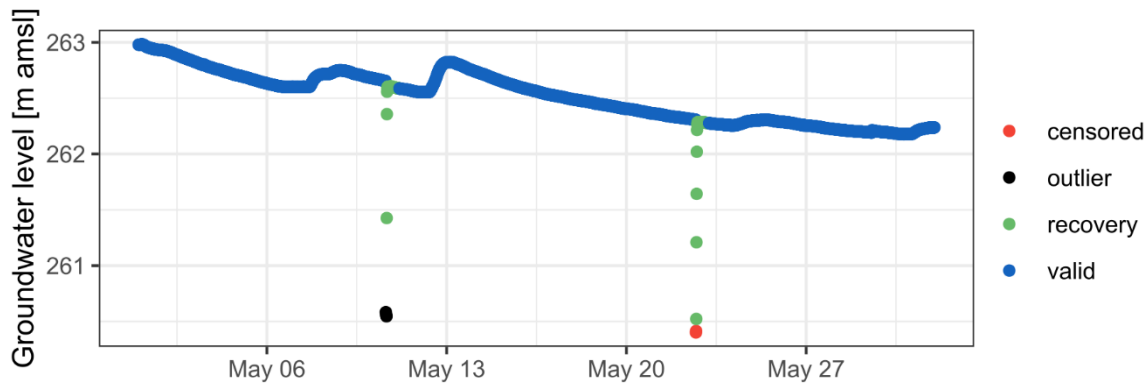
Figure 6: Example of a groundwater time series (well A12, May 2019) affected by two pumping events, with identification of the outliers (black) during the time that the logger was outside the well (while the pumping took place) and the recovery period (green). Water levels below the threshold of 5 cm above the logger end are classified as censored (red).

To download the loggers, take manual water level measurements, or purge the wells for cleaning and sampling (see description of Dataset 2), the loggers were taken out of the wells. This usually took a short time, and therefore, the loggers were not stopped. Most of the measurements taken during these periods were significantly lower than those taken before or afterwards and are consequently classified as *outlier*s. To find these outliers, we used a filter based on the changes in the water levels. Assuming that groundwater levels generally do not drop abruptly (i.e., the recession is smooth), we used a threshold value of a more than 10 cm drop in groundwater level within 10 min to find outliers. These outliers were then manually investigated to ensure correct identification.

Data points collected after the re-introduction of the logger into the well after well purging were classified as *recovery* to mark the time of recovery of the water level within the well. To be sure that equilibrium had been reached, all data points within 12 hours after the re-insertion of the logger to the well were classified as recovery. Where the recovery time appeared to exceed the 12-hour time span, we extended the classification to 24 hours after re-introduction of the logger.

When the groundwater level was close to the weight at the end of the sensor cable, the recorded data often showed sudden jumps, suggesting a low accuracy of the measurements. To eliminate this problem and the problem of standing water in the very bottom of the well (which was not screened), we classified all points that were less than 5 cm above the logger end as *censored*.

For five wells of the 74 wells (A21, A9, A4, B1, and B6), we observed a continuous drop in the water level between 21.04.2019 and 30.04.2019 (see examples in Figure 7). We expect the groundwater level

360 to rise, rather than drop for this peak snowmelt period. The start of the drop in the water level differed for the wells, but it ended suddenly for all five wells on 30.04.2019, when the loggers were removed from the wells to download the data. After the re-introduction of the loggers in the wells, the measured water levels were several centimeters higher than before. The logger string or tube lengths were not adjusted during this period and the sudden change in the recorded water level can not be related to errors

365 in these measurements. The wells for which this strange behavior was observed were not located in one region or characterized by a particular topographic position either. These were all located close to other groundwater wells (within ~ 5 m), for which we did not observe such a change. Therefore, the data from these wells during this period are flagged as *strange*. Because the recorded time series after the re-introduction of the loggers to the well seems to agree with the water levels observed in the days before

370 the sudden drop, we expect that the lowering of Electrical Conductivity (EC) of the water in the wells due to the infiltration of low EC meltwater caused this change. Odyssey water level logger recordings can be sensitive to a large change in EC (Larson and Runyan, 2009). Most probably, the removal of the logger from the well and its re-introduction stirred the water inside the wells and led to the mixing of the snow meltwater and older groundwater. The alternative explanation of a film (biological or other)

375 on the cables does not correspond with our field notes. Only in two cases was a film observed on the sensor cables, but for these sensors, the logged values seem to be normal during this period.
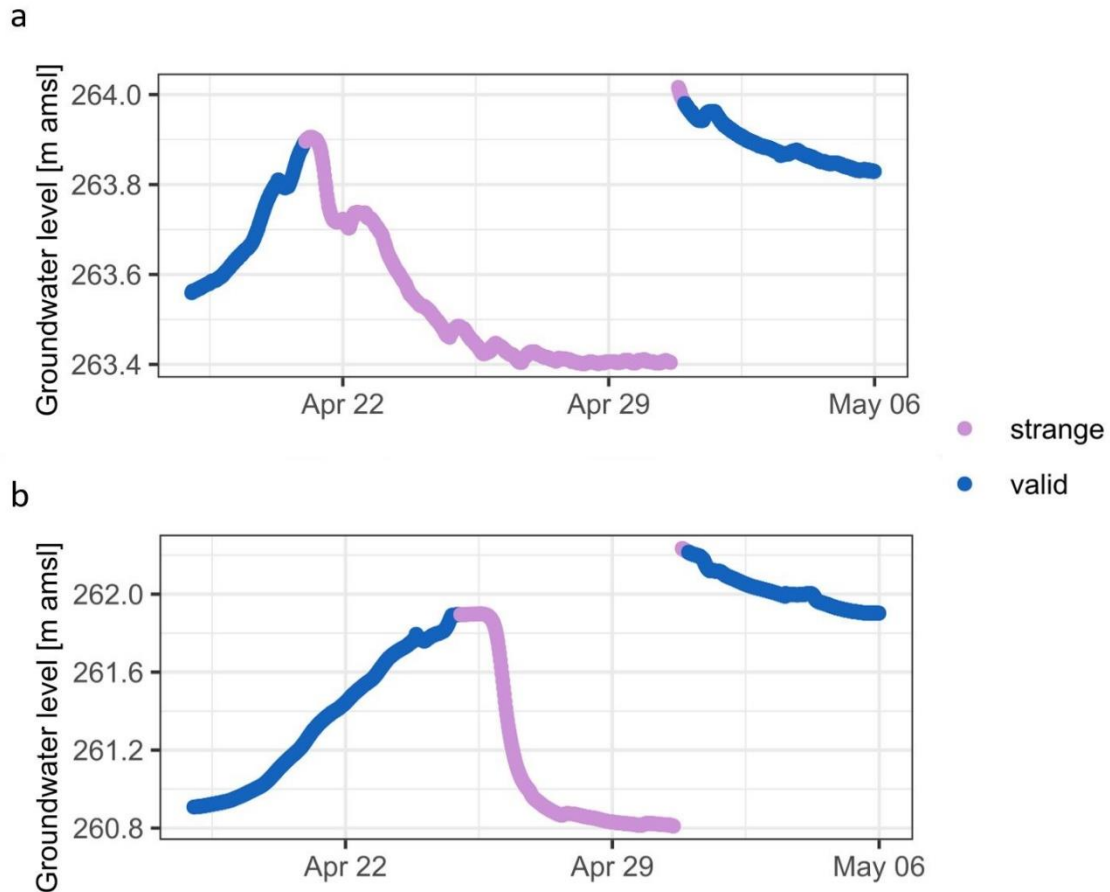
Figure 7: Examples of strange drops in the measured water level during the 2019 spring melt period for two wells (well A4 (a) and well A21 (b)).

5. Dataset 2: Groundwater chemistry

5.1 Dataset structure

In the summer of 2019, a groundwater sampling campaign was undertaken to obtain spatially distributed information on groundwater chemistry. The resulting groundwater chemistry dataset (Dataset 2) consists of four files. One file (Krycklan_sampling.csv) provides a description of each sample (Table 2) and another one (Krycklan_chemistry.csv) the laboratory results for each sample (see Table A 6 for a description of its structure). The third file contains the field protocol (Field_protocol.csv), and the fourth file (Lab_analysis_description.pdf) provides additional details on the laboratory analyses. The sampling and data analyses are described in more detail in the following sections.

Table 2: Description of groundwater sampling data (file: 2022-020_Erdbruegger-et-al_Krycklan_sampling.csv)

Column name	Full title	Description [unit]
Well	Well name	Name of the sampled well
sample	Upper [1] or lower [2] sample within well	Upper (first [1]) or lower (second [2]) sample from well. If only one sample was taken, it was also noted as upper (first [1]) sample
Depth	Depth of sample	Sample depth (midpoint of the sample depth,) in absolute elevation [m amsl]
date	Date of sample	Date the sample was taken [DD/MM/YYYY]
sample_num	Sample number	Sample number assigned for SLU laboratory analysis
wl	Water level	Water level measured manually directly before sample extraction [m amsl], corresponds to mnl_level in Dataset 1.
quality	Sample quality	First impression in field of sample quality (turbidity/suspended sediment, air intrusion in sampling tube, etc.) [g] = Good, [d] = Doubtful (possible influence of aeration on the sample), [b] = Bad (influence of sediment or aeration on the water sample)

5.2 Sampling

The groundwater sampling was done between July 19th and 31st, 2019. Total precipitation during the sampling period in July was relatively low (28 mm in total, max. daily precipitation 13 mm). The sampling procedure and field protocol used for the campaign followed the Svartberget research station and Swedish University of Agricultural Sciences (SLU) standard procedure for groundwater sampling (see also the 2022-020_Erdbruegger-et-al_Field_protocol.csv-file). To ensure that the water samples were representative of the local groundwater, we did two rounds of purging with a peristaltic pump (see Figure A 2) between the middle (shortly after peak snowmelt) and the end of May 2019 (when groundwater levels were generally lower than for the first round). During both rounds, the wells were either pumped dry or at least three times the well volume (see Appendix B) was pumped out to ensure full replacement of the well water with "fresh" groundwater. The pumping also removed the sediment and other particles from the wells.

A custom-made straddle packer system with inflatable rubber tubes (see Appendix B, Figure A 3) allowed us to isolate a specific part of the well and sample water from a roughly 25 cm long interval. We aimed to obtain two samples per well: one sample just below the groundwater table (which would correspond to the uppermost portion of the groundwater at the respective location) and another sample from the deepest part of the well. Because many wells were shallow and groundwater levels were low at the end of July, there was insufficient water for two samples for many wells. In these cases, we took only one water sample from the deepest point of the well.

The pumping was done slowly (regulated manually) to not draw water from above, allow for recharge, and avoid excessive aeration of the samples. However, in some cases, the recharge of the wells was so slow that even the lowest pumping rate was too high, and the water level in the well dropped, or the well was pumped dry and aeration of the samples took place. When aeration occurred, it was noted in the sampling protocol as a qualitative indication that sample quality might be doubtful (d) or even bad (b) (see Table 2: quality; Sample quality). Prior to taking the actual sample, the tubes were flushed with ~2 L of well water to reduce cross-contamination of samples. The sample bottles were rinsed three times before filling them to the top, without air bubbles. Additionally, we measured the electrical conductivity (EC) and pH in the field with a pH/Cond 3320 sensor (Xylem Analytics Germany GmbH).

5.3 Lab analyses

The samples were analyzed for: EC, pH, absorbance at 254 nm, 365 nm, 420 nm, and 436 nm, anion (F, Cl, S-SO$_4$) concentrations, nutrient (P-PO$_4$, N-NH$_4$, N-NO$_3$) concentrations, and stable isotopes (δ^{18}O and δ^2H) in the laboratory of SLU, Sweden. The cation (Na, NH$_4$, K, Mg, Ca) concentrations were analyzed at the Hydrogeological Laboratory of the TU Bergakademie Freiberg, Germany. A detailed description of the lab procedures is given in the file: 2022-020_Erdbruegger-et-al_Lab_analysis_description.docx.
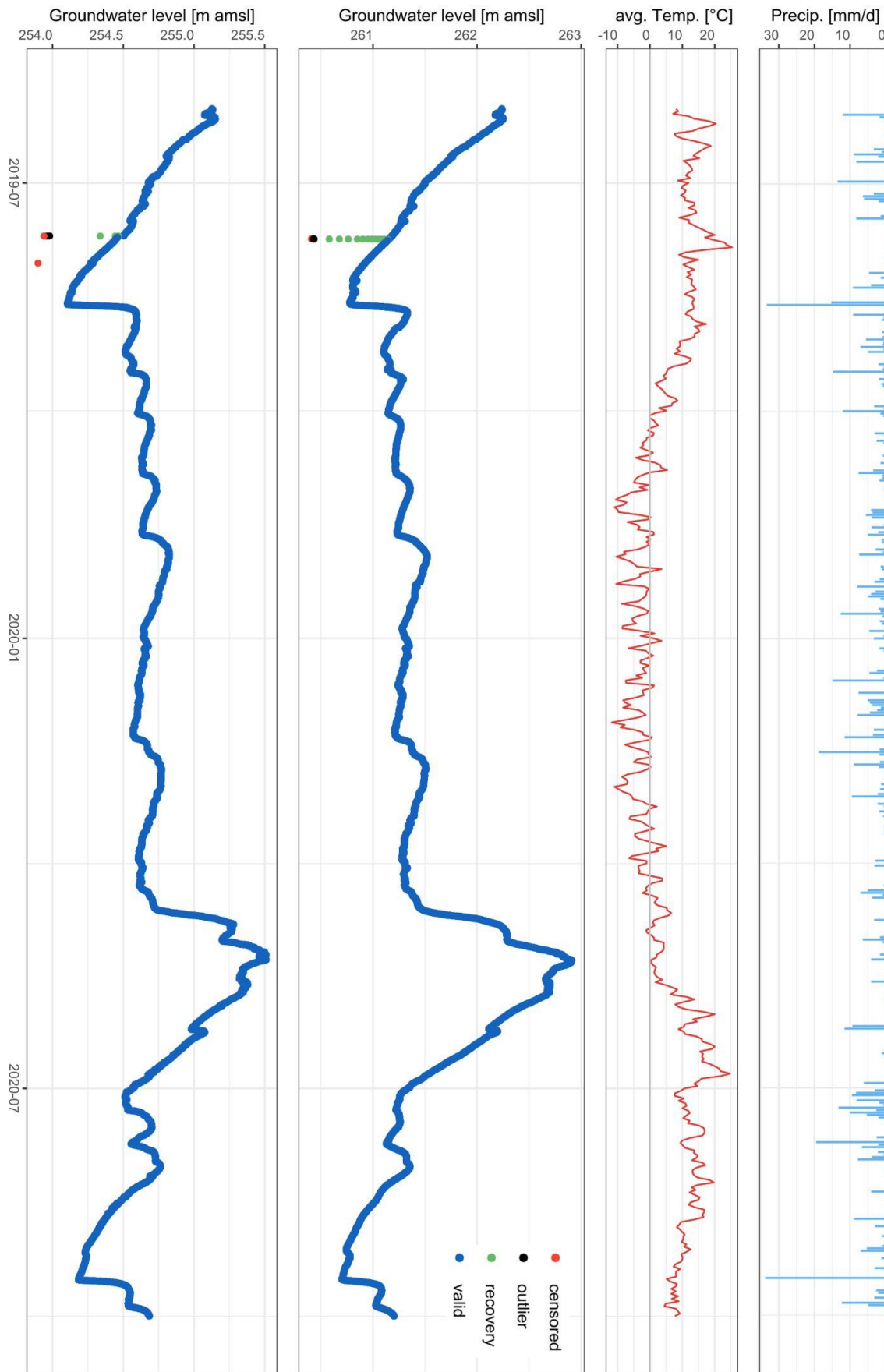
Figure 8: Precipitation (first plot, blue bars), temperature (daily average, second plot, red line) and classified groundwater levels for two wells (A12 third plot, B18 fourth plot) between June 2019 and September 2020. See Table A 5 for further information on the classification of the data points.

430

6. Example results

6.1 Groundwater level data

Figure 8 shows the groundwater level time series for two selected wells (A12 and B18) and highlights the quick response to snowmelt and rainfall events. Thanks to the relatively high resolution of the groundwater data, the immediate response of groundwater levels to specific rainfall events is clear. Interesting dynamics like daily groundwater level variations due to snowmelt, with peak water levels occurring during the early evening (see examples in Figure 9 (a)) and due to evapotranspiration with groundwater levels dropping during the day and stabilizing at night (see examples Figure 9 (b)) can also be observed for most wells (cf. Kirchner et al., 2020).
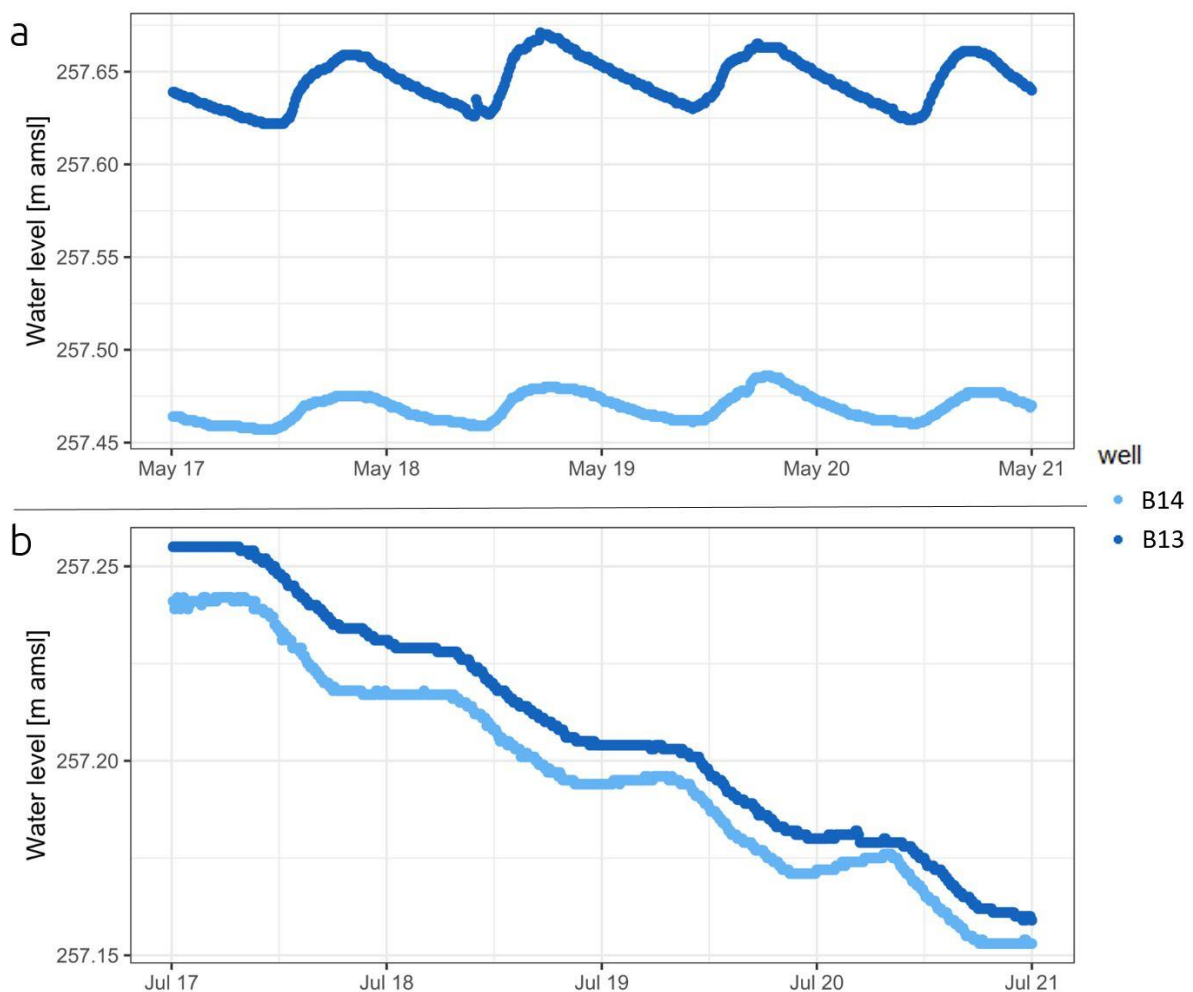
Figure 9: Example time series of diurnal variations in groundwater levels for two wells during the late snow melt period in May 2020 (a) and the summer (July 2020) when diurnal variations are caused by evapotranspiration (b).

6.2 Groundwater chemistry

The concentrations of the anions, cations, and nutrients in the groundwater are comparable to those reported from other measurements in the Krycklan catchment (e.g., Kolbe et al., 2020; Laudon et al.,

2013, 2021), but the spatial variation in the concentrations was large (cf. Kiewiet et al., 2020), with the coefficient of variation ranging from 2.5% (for $\delta^{18}O$) to 239% (for F) (see examples Figure 10 and Figure 11). The concentrations for the lower groundwater samples differed from those of the upper groundwater samples for most locations (e.g., Figure 10), but no clear trends could be identified. The isotopic composition of the groundwater was also variable, with the δ^2H, for example, varying by 12.5‰ for the groundwater samples taken near the groundwater table (Figure 11).

450
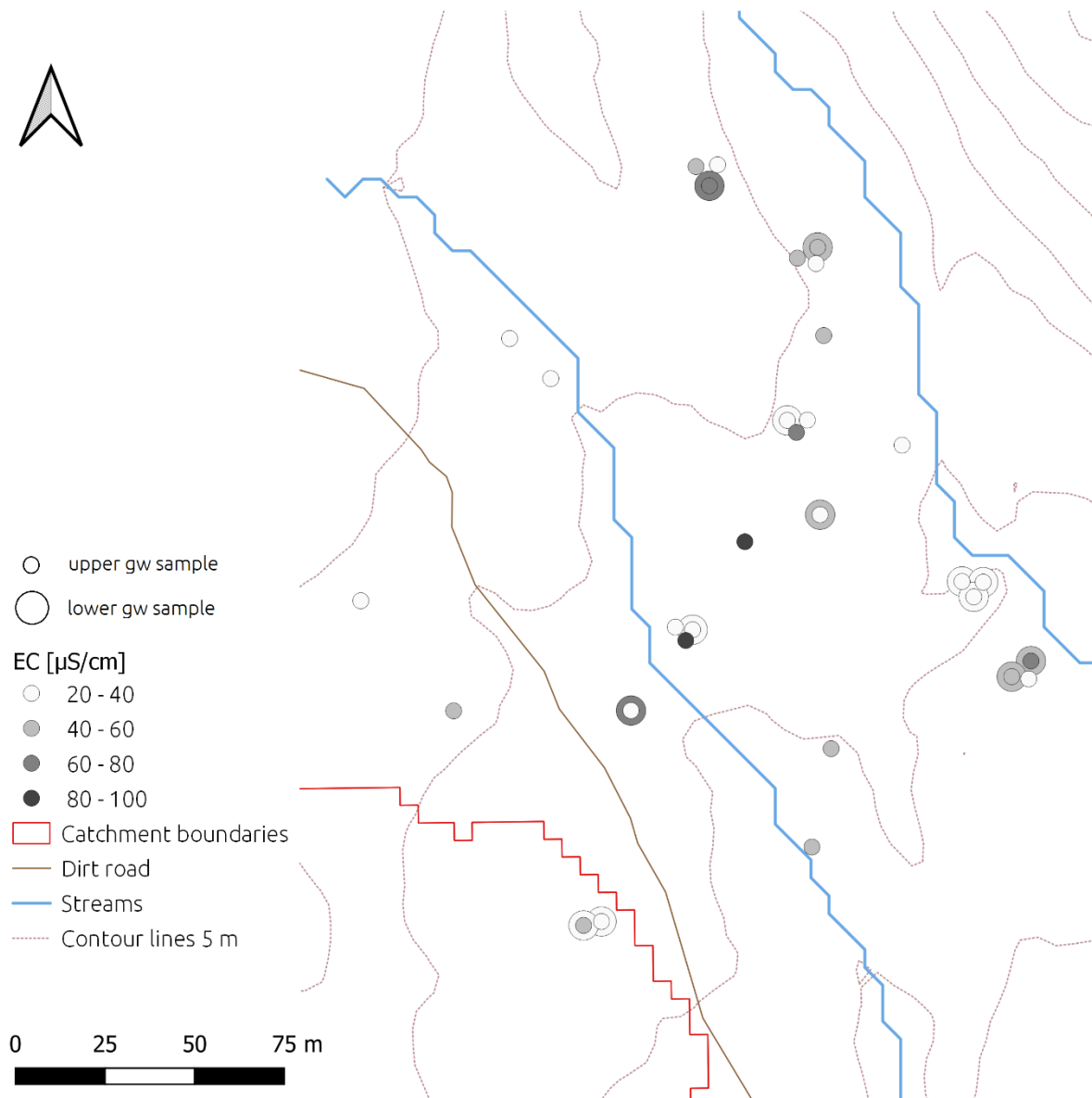
455 **Figure 10. Map of the electric conductivity (EC) of the groundwater samples taken near the water table (small circle; upper gw sample) and the bottom of the well (larger circle; lower gw sample) for the wells in study area A (also know as the C6 catchment). Where two circles are shown, the outer circle represents the groundwater sample taken from the bottom of the well and the inner circle the groundwater near the water table.**
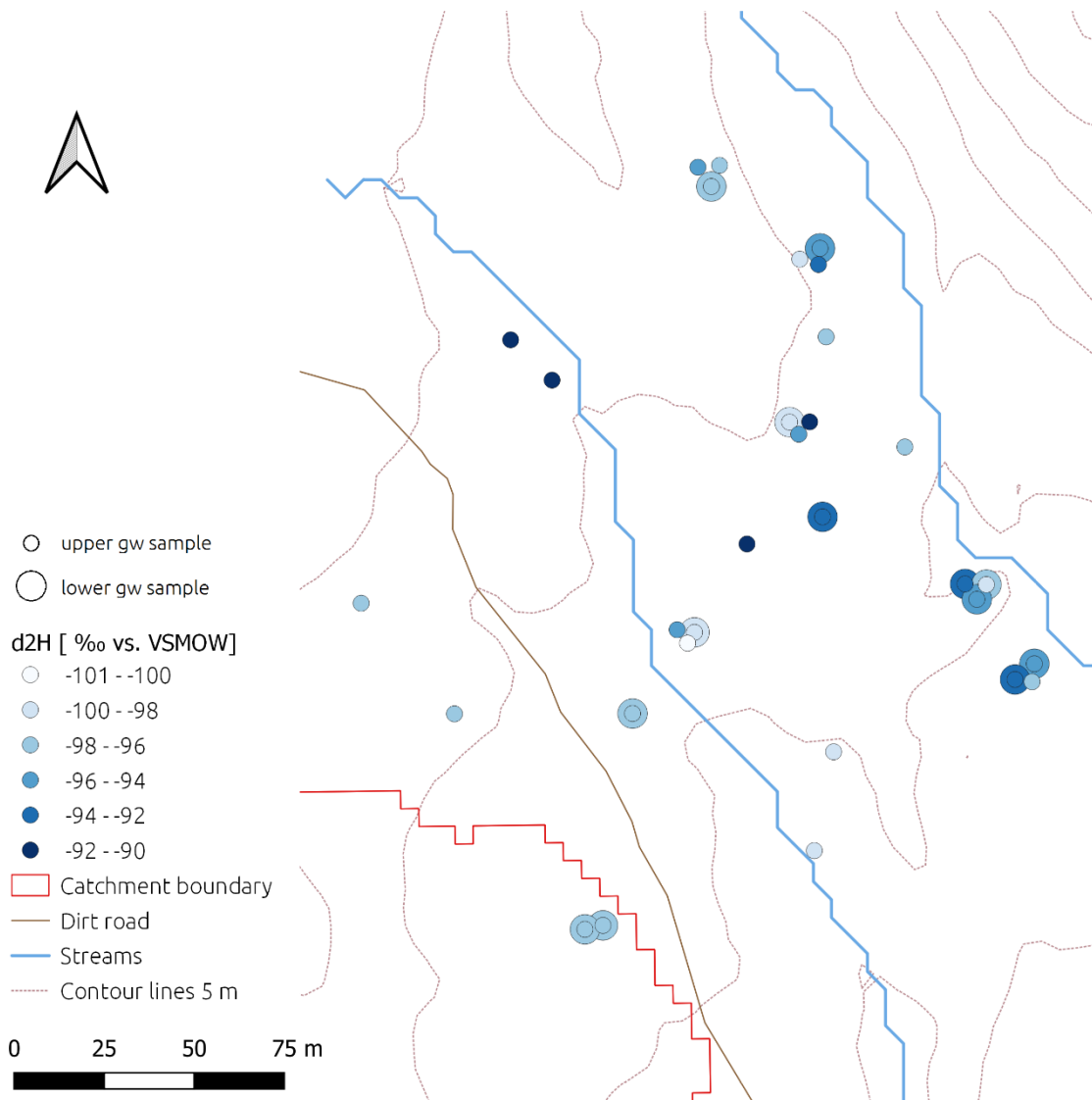
460 **Figure 11: Map of δ²H of the groundwater samples taken near the water table (small circle; upper gw sample) and the bottom of the well (larger circle; lower gw sample) for the wells in study area A (also know as the C6 catchment). Where two circles are shown, the outer circle represents the groundwater sample taken from the bottom of the well and the inner circle the groundwater near the water table.**

7. Concluding remarks

465 The datasets presented in this paper can be used to investigate the spatial and temporal dynamics of shallow groundwater and to test hydrological models or upscaling approaches. These data can be used in other studies in the Krycklan catchment to understand better its hydrological functioning or geochemical or ecological processes. The highly instrumented sites within the Krycklan catchment provide unique opportunities to study groundwater dynamics and the potential findings are relevant for

470 other boreal catchments. The wells are still in place and accessible. Thus, there is the possibility for continued groundwater level measurements and repeated sampling.

8. Data Availability

Dataset 1 and 2 can both be accessed and downloaded via https://doi.org/10.5880/fidgeo.2022.020 (Erdbrügger et al., 2022). The zip-compressed folder (2022-020_Erdbruegger-et-al_Krycklan_Groundwater_levels_sampling.zip) includes all the files listed in Table A 2. A brief description of the data and information on licensing and the format of the tabular data is available from 2022-020_Erdbruegger-et-al_data-description.pdf (available separately and within the zip-folder).

9. Author contribution

JE, IvM, JS and KB designed the experiments, JE led the installation of the wells, field measurements, recording of the water levels, and sampling. JE prepared the manuscript and data files with contributions from all co-authors.

10. Competing interests

The authors declare that they have no conflict of interest

11. Acknowledgements

We thank everyone involved in the installation and maintenance of the wells, especially Tommy Andersson, Alexandre Constan, Olivier Dulouard, Corentin Leprince, Johannes Larson, Ola Olafson, Paul Pister, Viktor Sjöblom, Jacob Smeds, Johannes Tiwari, and Jean-Thomas Wenner. We also thank SITES and SLU Umea for granting access to the area and research station and providing field equipment. Furthermore, we thank Hjalmar Laudon, Ida Manfredson, Charlotta Erefur and the entire Svartberget field research station crew for all the help with logistics and moral support during the fieldwork. The installation of the groundwater wells was made possible by funding from SKB (Svensk Kärnbränslehantering AB) and the SLU Excellence award to Hjalmar Laudon.

References

Ameli, A. A., Laudon, H., Teutschbein, C. and Bishop, K.: Where and When to Collect Tracer Data to Diagnose Hillslope Permeability Architecture, Water Resour. Res., 57(8), 1–21, doi:10.1029/2020WR028719, 2021.

Bachmair, S., Weiler, M. and Troch, P. A.: Intercomparing hillslope hydrological dynamics: Spatio-temporal variability and vegetation cover effects, Water Resour. Res., 48(5), 1–18, doi:10.1029/2011WR011196, 2012.

Bergsten, U., Goulet, F., Lundmark, T. and Ottosson Löfvenius, M.: Frost heaving in a boreal soil in relation to soil scarification and snow cover, Can. J. For. Res., 31(6), 1084–1092 [online] Available from: https://doi.org/10.1139/x01-042, 2001.

Beven, K. J. and Kirkby, M. J.: A physically based, variable contributing area model of basin hydrology, Hydrol. Sci. Bull., 24(1), 43–69, doi:10.1080/02626667909491834, 1979.

Bishop, K., Seibert, J., Nyberg, L. and Rodhe, A.: Water storage in a till catchment. II: Implications of transmissivity feedback for flow paths and turnover times, Hydrol. Process. [online] Available from: https://doi.org/10.1002/hyp.8355, 2011.

Bishop, K. H., Grip, H. and O'Neill, A.: The origins of acid runoff in a hillslope during storm events, J. Hydrol., 116(1–4), 35–61 [online] Available from: https://doi.org/10.1016/0022-1694(90)90114-D, 1990.

Bohlin, J. and Nyström, M.: Terrestrial laser scanning - Postprocessing a multiscan using 230 mm balls on the tripods, Ljungbergslaboratoriet - SLU [online] Available from: http://www.rslab.se/terrestrial-laser-scanning/#postprocessingGeoreferencing (Accessed 5 November 2019), 2019.

Bonanno, E., Blöschl, G. and Klaus, J.: Flow directions of stream-groundwater exchange in a headwater catchment during the hydrologic year Running head : Stream-groundwater exchange during the hydrologic year, Hydrol. Process., 0–2, doi:10.1002/hyp.14310, 2021.

Buffam, I., Laudon, H., Berggren, M., Anneli, A., Bishop, K., Grabs, T., Jansson, M. and Ko, S.: Patterns and Dynamics of Dissolved Organic Carbon (DOC) in Boreal Streams : The Role of Processes , Connectivity , and Scaling, , doi:10.1007/s10021-011-9452-8, 2011.

Condon, L. E. and Maxwell, R. M.: Water Resources Research, Water Resour. Res., 51, 6602–6621, doi:10.1111/j.1752-1688.1969.tb04897.x, 2015.

Covino, T. P. and McGlynn, B. L.: Stream gains and losses across a mountain-to-valley transition: Impacts on watershed hydrology and stream water chemistry, Water Resour. Res., 43(10), 1–14, doi:10.1029/2006WR005544, 2007.

Dataflow Systems Ltd: Odyssey Capacitance Water Level Logger, [online] Available from: http://odysseydatarecording.com/index.php?route=product/product&path=59&product_id=50, 2021.

Dataflow Systems PTY Limited: Technical Handbook for Odyssey Data Logger, 2012.

Doering, M., Uehlinger, U., Rotach, A., Schlaepfer, D. R. and Tockner, K.: Ecosystem expansion and contraction dynamics along a large Alpine alluvial corridor (Tagliamento River, Northeast Italy), Earth Surf. Process. Landforms, 32, 1693–1704, doi:10.1002/esp, 2007.

Drive, S.: Trimble TX6 / TX8, 3D Laser Scanner, User Guide, 1st ed., Trimble Inc., Sunnyvale, USA., 2017.

Eklöf, K., Kraus, A., Futter, M., Schelker, J., Meili, M., Boyer, E. W. and Bishop, K.: Parsimonious Model for Simulating Total Mercury and Methylmercury in Boreal Streams Based on Riparian Flow Paths and Seasonality, Environ. Sci. Technol., 49(13), 7851–7859, doi:10.1021/acs.est.5b00852, 2015.

Erdbrügger, J., van Meerveld, I., Bishop, K. and Seibert, J.: Effect of DEM-smoothing and -aggregation on topographically-based flow directions and catchment boundaries, J. Hydrol., 602(November 2020), 126717, doi:10.1016/j.jhydrol.2021.126717, 2021.

Erdbrügger, J., van Meerveld, I., Seibert, J. and Bishop, K.: Shallow groundwater level time series and

groundwater chemistry survey data from Krycklan catchment, GFZ Data Serv. [online] Available from: https://doi.org/10.5880/fidgeo.2022.020, 2022.

Fan, Y.: Are catchments leaky?, WIREs Water, 6(6), 1–25, doi:10.1002/wat2.1386, 2019.

Fan, Y. and Schaller, M. F.: River basins as groundwater exporters and importers: Implications for water
545   cycle and climate modeling, J. Geophys. Res. Atmos., 114(4), doi:10.1029/2008JD010636, 2009.

Gabrielli, C. P. and Mcdonnell, J. J.: An inexpensive and portable drill rig for bedrock groundwater studies in headwater catchments, Hydrol. Process., 26(4), 622–632, doi:10.1002/hyp.8212, 2012.

Guaraglia, D. O. and Pousa, J. L.: Water Level and Groundwater Flow Measurements, in Introduction to Modern Instrumentation. For Hydraulics and Environmental Sciences, De Gruyter, Berlin, Boston.,
550   2014.

Haitjema, H. M. and Mitchell-Bruker, S.: Are water tables a subdued replica of the topography?, Ground Water, 43(6), 781–786, doi:10.1111/j.1745-6584.2005.00090.x, 2005.

ICOS: Svartberget, [online] Available from: https://www.icos-sweden.se/Svartberget, 2021.

Ivarsson, H.: Glacial dynamics and till genesis in hilly terrain: A study in the Tallträsk area, central-
555   northern Sweden., 2007.

Ivarsson, H. and Johnsson, T.: Quaternary deposits in Svartberget, 1988.

Jencso, K. G., McGlynn, B. L., Gooseff, M. N., Wondzell, S. M., Bencala, K. E. and Marshall, L. A.: Hydrologic connectivity between landscapes and streams: Transferring reach- and plot-scale understanding to the catchment scale, Water Resour. Res., 45(4), 1–16, doi:10.1029/2008WR007225,
560   2009.

Jutebring Sterte, E.: Integrated Hydrologic Flow Characterization of the Krycklan Catchment, KTH Royal Institute of Technology Architecture., 2016.

Kiewiet, L., Freyberg, J. and Meerveld, H. J. (Ilja): Spatiotemporal variability in hydrochemistry of shallow groundwater in a small pre-alpine catchment: The importance of landscape elements, Hydrol.
565   Process., 33(19), 2502–2522, doi:10.1002/hyp.13517, 2019.

Kiewiet, L., van Meerveld, I., Stähli, M. and Seibert, J.: Do streamwater solute concentrations reflect when connectivity occurs in a small pre-alpine headwater catchment?, Hydrol. Earth Syst. Sci. Discuss., (2011), 1–25, doi:10.5194/hess-2019-686, 2020.

Kirchner, J., Godsey, S., Osterhuber, R., McConnell, J. and Penna, D.: The pulse of a montane
570   ecosystem: coupled daily cycles in solar flux, snowmelt, transpiration, groundwater, and streamflow at Sagehen and Independence Creeks, Sierra Nevada, USA, Hydrol. Earth Syst. Sci. Discuss., 1–46, doi:10.5194/hess-2020-77, 2020.

Kolbe, T., Marçais, J., de Dreuzy, J. R., Labasque, T. and Bishop, K.: Lagged rejuvenation of groundwater indicates internal flow structures and hydrological connectivity, Hydrol. Process., 34(10),
575   2176–2189, doi:10.1002/hyp.13753, 2020.

Larson, P. and Runyan, C.: Evaluation of a Capacitance Water Level Recorder and Calibration Methods in an Urban Environment, CUERE Tech. Memo, (September), 36 [online] Available from:

http://www.umbc.edu/cuere/BaltimoreWTB/pdf/TM_2009_003.pdf, 2009.

Laudon, H., Taberman, I., Ågren, A., Futter, M., Ottosson-Löfvenius, M. and Bishop, K.: The Krycklan

580   Catchment Study - A flagship infrastructure for hydrology, biogeochemistry, and climate research in the
boreal landscape, Water Resour. Res., 49(10), 7154–7158, doi:10.1002/wrcr.20520, 2013.

Laudon, H., Hasselquist, E. M., Peichl, M., Lindgren, K., Sponseller, R., Lidman, F., Kuglerová, L.,
Hasselquist, N. J., Bishop, K., Nilsson, M. B. and Ågren, A. M.: Northern landscapes in transition:
Evidence, approach and ways forward using the Krycklan Catchment Study, Hydrol. Process., 35(4), 1–

585   15, doi:10.1002/hyp.14170, 2021.

Ledesma, J. L. J., Futter, M. N., Blackburn, M., Lidman, F., Grabs, T., Sponseller, R. A., Laudon, H.,
Bishop, K. H. and Köhler, S. J.: Towards an Improved Conceptualization of Riparian Zones in Boreal
Forest Headwaters, Ecosystems, 21(2), 297–315, doi:10.1007/s10021-017-0149-5, 2018.

Lindgren,   K.:   The   Krycklan   Infrastructure,   [online]   Available   from:

590   https://www.slu.se/en/departments/field-based-forest-research/experimental-forests/vindeln-
experimental-forests/krycklan/infrastructure/, 2021.

Lyon, S. W., Nathanson, M., Spans, A., Grabs, T., Laudon, H., Temnerud, J., Bishop, K. H. and Seibert,
J.: Specific discharge variability in a boreal landscape, Water Resour. Res., 48(8), 1–13,
doi:10.1029/2011WR011073, 2012.

595   van Meerveld, H. J., Seibert, J. and Peters, N. E.: Hillslope-riparian-stream connectivity and flow
directions at the Panola Mountain Research Watershed, Hydrol. Process., 29(16), 3556–3574,
doi:10.1002/hyp.10508, 2015.

Moore, R. D. and Thompson, J. C.: Are water table variations in a shallow forest soil consistent with
the TOPMODEL concept?, Water Resour. Res., 32(3), 663–669, doi:10.1029/95WR03487, 1996.

600   Munthe, J. and Hultberg, H.: Mercury and methylmercury in runoff from a forested catchment -
Concentrations, fluxes, and their response to manipulations, Water, Air, Soil Pollut. Focus, 4(2–3), 607–
618, doi:10.1023/B:WAFO.0000028381.04393.ed, 2004.

Murphy, P. N. C., Ogilvie, J. and Arp, P.: Topographic modelling of soil moisture conditions: A
comparison and verification of two models, Eur. J. Soil Sci., 60(1), 94–109, doi:10.1111/j.1365-

605   2389.2008.01094.x, 2009.

Myrabø, S.: Temporal and spatial scale of response area and groundwater variation in till, Hydrol.
Process., 11(14), 1861–1880, doi:10.1002/(sici)1099-1085(199711)11:14<1861::aid-hyp535>3.0.co;2-
p, 1997.

Panneer Selvam, B., Laudon, H., Guillemette, F. and Berggren, M.: Influence of soil frost on the

610   character and degradability of dissolved organic carbon in boreal forest soils, J. Geophys. Res.
Biogeosciences, 121(3), 829–840, doi:10.1002/2015JG003228, 2016.

Payn, R. A., Gooseff, M. N., McGlynn, B. L., Bencala, K. E. and Wondzell, S. M.: Channel water
balance and exchange with subsurface flow along a mountain headwater stream in Montana, United
States, Water Resour. Res., 45(11), doi:10.1029/2008WR007644, 2009.

615   Penna, D. and van Meerveld, H. J.: Spatial variability in the isotopic composition of water in small catchments and its effect on hydrograph separation, Wiley Interdiscip. Rev. Water, 6(5), 1–33, doi:10.1002/wat2.1367, 2019.

Ploum, S. W., Laudon, H., Peralta-tapia, A. and Kuglerová, L.: Are dissolved organic carbon concentrations in riparian groundwater linked to hydrological pathways in the boreal forest ?, Hydrol.

620   Earth Syst. Sci., 24, 1709–1720, 2020.

Rau, G. C., Post, V. E. A., Shanafield, M., Krekeler, T., Banks, E. W. and Blum, P.: Error in hydraulic head and gradient time-series measurements: A quantitative appraisal, Hydrol. Earth Syst. Sci., 23(9), 3603–3629, doi:10.5194/hess-23-3603-2019, 2019.

Retike, I., Bikše, J., Kalvāns, A., Dēliņa, A., Avotniece, Z., Zaadnoordijk, W. J., Jemeljanova, M.,

625   Popovs, K., Babre, A., Zelenkevičs, A. and Baikovs, A.: Rescue of groundwater level time series: How to visually identify and treat errors, J. Hydrol., 605(June 2021), doi:10.1016/j.jhydrol.2021.127294, 2022.

Rinderer, M., van Meerveld, I. and Seibert, J.: Topographic controls ond shallow groundwater levels in a steep, prealpine catchment, Water Resour. Res., 50, 6067–6080, doi:10.1002/2013WR015009, 2014.

630   Rinderer, M., van Meerveld, H. J. and McGlynn, B. L.: From Points to Patterns: Using Groundwater Time Series Clustering to Investigate Subsurface Hydrological Connectivity and Runoff Source Area Dynamics, Water Resour. Res., 55(7), 5784–5806, doi:10.1029/2018WR023886, 2019.

Rodhe, A. and Seibert, J.: Groundwater dynamics in a till hillslope: Flow directions, gradients and delay, Hydrol. Process., 25(12), 1899–1909, doi:10.1002/hyp.7946, 2011.

635   Seibert, J., Bishop, K., Rodhe, A. and McDonnell, J. J.: Groundwater dynamics along a hillslope: A test of the steady state hypothesis, Water Resour. Res., 39(1), 1–9, doi:10.1029/2002WR001404, 2003.

Seibert, J., Bishop, K., Nyberg, L. and Rodhe, A.: Water storage in a till catchment. I: Distributed modelling and relationship to runoff, Hydrol. Process., 25(25), 3937–3949, doi:10.1002/hyp.8309, 2011.

640   Simpson, S. C. and Meixner, T.: The influence of local hydrogeologic forcings on near-stream event water recharge and retention (Upper San Pedro River, Arizona), Hydrol. Process., 27(4), 617–627, doi:10.1002/hyp.8411, 2013.

Sponseller, R. A., Gundale, M. J., Futter, M., Ring, E., Nordin, A., Näsholm, T. and Laudon, H.: Nitrogen dynamics in managed boreal forests: Recent advances and future research directions, Ambio,

645   45, 175–187, doi:10.1007/s13280-015-0755-4, 2016.

Tóth, J.: A Theory of Groundwater Motion in Small Drainage Basins, J. Geophys. Res., 67(11), 1962.

Tromp-van Meerveld, H. J. and McDonnell, J. J.: Threshold relations in subsurface stormflow: 1. A 147-storm analysis of the Panola hillslope, Water Resour. Res., 42(2), 1–11, doi:10.1029/2004WR003778, 2006.

650   Vidon, P.: Towards a better understanding of riparian zone water table response to precipitation: Surface water infiltration, hillslope contribution or pressure wave processes?, Hydrol. Process., 26(21), 3207–

3215, doi:10.1002/hyp.8258, 2012.

Ward, A. S., Payn, R. A., Gooseff, M. N., McGlynn, B. L., Bencala, K. E., Kelleher, C. A., Wondzell, S. M. and Wagener, T.: Variations in surface water-ground water interactions along a headwater mountain stream: Comparisons between transient storage and water balance analyses, Water Resour. Res., 49(6), 3359–3374, doi:10.1002/wrcr.20148, 2013.

Winter, T. C.: Relation of streams, lakes, and wetlands to groundwater flow systems, Hydrogeol. J., 7(1), 28–45, doi:10.1007/s100400050178, 1999.

Yu, M. C. L., Cartwright, I., Braden, J. L. and De Bree, S. T.: Examining the spatial and temporal variation of groundwater inflows to a valley-to-floodplain river using 222Rn, geochemistry and river discharge: The ovens river, southeast Australia, Hydrol. Earth Syst. Sci., 17(12), 4907–4924, doi:10.5194/hess-17-4907-2013, 2013.

Zimmer, M. A. and McGlynn, B. L.: Bidirectional stream–groundwater flow in response to ephemeral and intermittent streamflow and groundwater seasonality, Hydrol. Process., 31(22), 3871–3880, doi:10.1002/hyp.11301, 2017.

Table A 1: Selected catchment and hillslope scale studies with a large number of shallow groundwater level measurements and reported well densities (number of wells per hectare).

Catchment	Recording wells		Manual measurements		Reference
	#	#/ha	#	#/ha	
Catchment studies					
Malcolm Knapp Research Forest, Canada	-	-	59	15	Moore and Thompson (1996)
Sæternbekken catchment, Norway	4		>100	0.01	Myrabø (1997)
Tenderfoot Creek Experimental Forest, Montana, USA	84	0.5	-		Jencso et al. (2009)
Östfora experimental catchment, Sweden	-		15	0.4	Rodhe and Seibert (2011)
Studibach catchment, Switzerland	51	2.6			Rinderer et al. (2014)
Near the Weierbach experimental catchment, Luxembourg.	22	195	14	125	Bonanno et al. (2021)
Krycklan catchment (C6, area A), Sweden	54	15	-		This study
Hillslope studies					
Panola Mountain Research Watershed trenched hillslope	29	29	135	135	Tromp-van Meerveld and McDonnell (2006)
Scott Starling Nature Sanctuary site/Riparian Zone	-		14	2.3	Vidon and Smith, (2007), Vidon (2012)
Malcom Knapp Research Forest, Canada	18	819	-		Haught and van Meerveld (2011)
Southern Germany	90	4.3	-		Bachmair, Weiler and Troch (2012)
Krycklan catchment (S-transect, area B), Sweden	20	20	-		This study
Gårdsjön Covered Catchment	3	4.8	34	54	Bishop et al. (2011), Seibert et al. (2011)

Table A 2: Name and short description of the datafiles included in the two datasets

Dataset	File names	Short description	Contents described in
1	2022-020_Erdbruegger-et-al_Krycklan_gw_wells.csv	well position (x,y,z), height of correction factors, etc.	Table A 3
1	2022-020_Erdbruegger-et-al_Krycklan_gw_levels.csv	Groundwater levels from manual measurements and loggers, tube above ground, etc.	Table A 4
1	2022-020_Erdbruegger-et-al_TSL_registration_report_[A/B].rtf	TSL scan registration report	Section 3.3
2	2022-020_Erdbruegger-et-al_Krycklan_gw_sampling.csv	Sampling information for groundwater chemistry	Table 2
2	2022-020_Erdbruegger-et-al_Krycklan_gw_chemistry.csv	Chemistry data from groundwater sampling	Table A 6
2	2022-020_Erdbruegger-et-al_Field_protocol.csv	Field protocol for sampling of groundwater	Section 5
2	2022-020_Erdbruegger-et-al_Lab_analysis_description.pdf	Information on the laboratory analyses	Section 5

 Appendix B

Table A 3: Structure of the groundwater well location data file (2022-020_Erdbruegger-et-al_Krycklan_gw_wells.csv) and description of the column names

Column name	Full title	Description
Well	Well_name	Name of well
Well_field	Well field name	Name of the well used in the field originally
X	X-Coordinate	X coordinate [m] as extracted from TLS Datum: EPSG:3006 - SWEREF99 TM
Y	Y-Coordinate	Y coordinate [m] as extracted from TLS Datum: EPSG:3006 - SWEREF99 TM
Z_abs	Z-tube top	Absolute elevation of pipe top above mean sea level extracted from TLS [m amsl]
Depth	Well depth	Depth of the well below the ground surface at the time of installation [m]
intercept	Recalibration offset	Recalibration offset calculated based on the linear regression between the manually measured water levels and the logger derived data, used to correct the logger measurements (only applied correction values)

Table A 4: Structure of the groundwater level data file (2022-020_Erdbruegger-et-al_Krycklan_gw_levels.csv) and
 description of the column names

Column name	Full title	Description [unit]
Well	Well_name	Name of well
datetime	Date and time	Date and time (CET) of the measurement Format: DD/MM/YYYY hh:mm:ss (no energy saving time)
tube	Length of the pipe above ground	Length of the PVC pipe above the ground [cm] as measured during field season (i.e., stick-up). Values are assumed to remain constant between measurements.
mnl_level	Manual water level	Groundwater level [m amsl], calculated by subtracting the manually measured distance between the water level and the top of the pipe (man_level) from the from the absolute elevation (Z_abs)
Log_level_uncorr	Water level below top of well (uncorrected)	Water level from logger [cm from the top of the tube], calculated based on the logger length and string length (if logger was suspended inside the well). Note that

		this is the level before the re-calibration with manually measured water levels
Log_level_corr	Absolute water level (corrected)	Water level after correction and subtraction from the absolute elevation (Z_abs) [m amsl]
Class	Data classification	Data point flagging as valid, outlier, recovery, etc. (see Table A 5)
Class_mnl	Manual Data classification	Manual data point flagging based on field observations (valid, outlier)

Appendix C

Table A 5: Classification of logged data points

Class	Description
Valid	No known or apparent reason to indicate that the measurement is not valid. This is the default classification for all data points
Outlier	Known outliers (during pumping) and unknown outliers (>10 cm drop in ≤10 min)
Recovery	Recovery of water levels after pumping (0-12 h after re-introduction of the logger into the well)
Censored	Uncertain values due to low water levels (< 5 cm above logger bottom) or water in lower well ends (lower 5 cm of unscreened pipe)
Strange	Snowmelt curve with sudden breaks (probably related to a rapid decrease in the electrical conductivity of the water)
Offset	String length or tube length were unknown. The relative changes in water level are correct but the absolute level could not be calculated.

685

Appendix D

Table A 6: Description of groundwater chemistry data (file: 2022-020_Erdbruegger-et-al_Krycklan_chemistry.csv), see Lab_analysis_description.pdf - file for more information on the laboratory analysis.

Column name	Full title or description	[units]
sample_num	Sample number assigned for SLU laboratory analysis	Sample number assigned for SLU laboratory analysis
d18O	$\delta^{18}O$	[‰ relative to VSMOW]
d2H	δ^2H	[‰ relative to VSMOW]
EC	Electrical conductivity EC	[μS/cm]
pH	pH	[-]
EC_field	Electrical conductivity measured in the field	μS/cm]
pH_field	pH measured in the field	[-]
absorb_254	Absorbance at 254 nm	[A/cm]
absorb_365	Absorbance at 365 nm	[A/cm]
absorb_420	Absorbance at 420 nm	[A/cm]
absorb_436	Absorbance at 436 nm	[A/cm]
Flu	Fluoride	[mg/L]
Cl	Chloride	[mg/L]
SSO4	Sulfate-SO_4	[mg/L]
PPO4	Phosphate-PO_4	[μg/L]
NNH4	Ammonium-NH_4	[μg/L]
NNO3	Nitrate-NO_3	[μg/L]
Na	Sodium	[mg/L]
NH4	Ammonium	[mg/L]
K	Potassium	[mg/L]
Mg	Magnesium	[mg/L]
Ca	Calcium	[mg/L]

690

Appendix E: Additional information on the water level measurements

E.1 Manual water level measurements

We used three different methods to measure the depth between the top of the well and the water level:
a bubbler, a water level plopper ("kluk lod"), and an acoustic water level sounder. The so-called
"bubbler" consists of a rigid tube connected to flexible tubing. In our case, we used a 1 m long metal
tube with a ~ 5mm diameter connected to flexible rubber tubing. The metal tube was inserted into the
well and air was blown into the flexible tube. The water level in the well was determined based on the
change in the sounds once the metal tube reached the water surface (i.e., as soon as one could hear a
"bubbling" noise). This method worked best for shallow groundwater levels since the sound was
difficult to discern when the water level was deeper (as well as in noisy circumstances (e.g., strong
winds)). Because the water can be blown out of the well when blowing too strongly, leading to a slightly
deeper groundwater level, we carefully approached the groundwater surface from above and provided
only moderate pressure.

A water-level plopper consists of a small metal cylinder attached to the tip of a measuring tape. It is
lowered into a well and produces a "plopping" sound when the cylinder hits the water surface. When
the water level was deep (>3 m), the sound was sometimes not audible. Also, for shallow groundwater
levels, it often took several tries and "plop" sounds to determine the exact depth to the water level with
the measuring tape because it required enough momentum for the cylinder to produce a sufficiently
distinguishable sound.

The electronic water level meter or (acoustic) water level sounder emits a sound upon contact with water.
In addition, a light switches on. The sensor at the tip of the tape or meter has an open electrical circuit
closed when it is in contact with water because of the much lower electric resistivity of water than air.
Because the groundwater in the Krycklan area has a relatively low electric conductivity (mean EC from
the surveys 48.6 µS/cm), the electronic water level meter sometimes failed and indicated the water
surface only after being submerged for about half a meter. The problem was solved after purging the
wells or stirring the water in the wells. The low EC in some wells may have originated from the
snowmelt water that did not drain or mix much with the other groundwater in the well.

E.2 Continuous water level measurements

We used Odyssey water level loggers for the continuous water level measurements. These capacitance
sensors are based on the difference in the dielectric constants of water and air. The weight at the end of
a cable serves as one capacitance plate, and the cable as the second. A change in the area of the second
capacitance plate (i.e., the cable in contact with the water) results in a change in the signal. For more
information on capacitance sensors, see Larson and Runyan (2009); Dataflow Systems PTY Limited
(2012); Guaraglia and Pousa (2014)). We deployed two generations of the same type of loggers, which
differ in their dimensions (Figure A 1 (a) and (c)). The new logger bodies (from 2019) are larger and do
not fit completely into the well pipes (see Figure A 1 (b) and (Figure A 1 (d)).

The water used for the calibration was taken from a groundwater well to account for local water chemistry (as this has been shown to be a potential error source by Larson and Runyan (2009)) and thus to minimize errors in the calibration. Other error sources identified by Larson and Runyan (2009), like the potential for a biofilm to build up on cable and counterweight of the loggers, were minimized by cleaning the cables and weights with a cloth during logger read-outs. The building of films varied strongly between wells but did not appear to have an identifiable impact in the data of the water levels and therefore we did not correct for this.

Since the loggers do not show the remaining battery power, it is relatively difficult to predict when they run out of power. Although a rough estimate says the batteries last for about 18 months, this time can vary considerably with environmental factors and is much shorter during low temperatures. This resulted in incomplete time series for some wells (see Table A 7 in Appendix C).
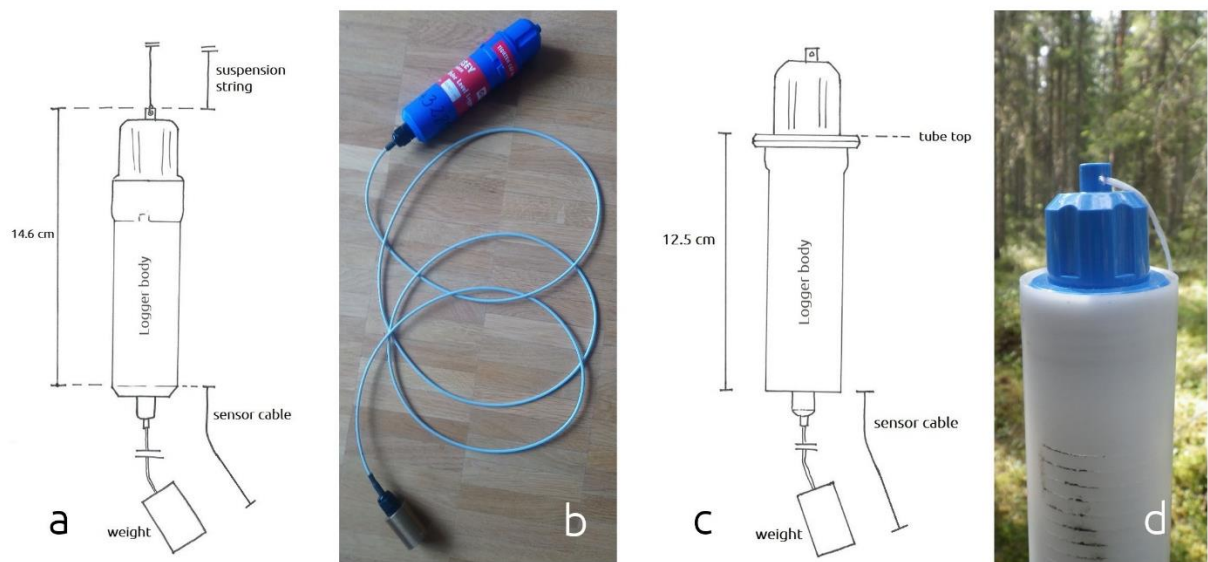
Figure A 1: Odyssey water level sensors and the respective measures of the logger body and cable lengths for the 2012 Odyssey water level sensor ((a) and (b)) and the 2019 Odyssey water level sensor (c), and the 2019 sensor installed in a well tube (d). Note, drawing is not to scale.

Appendix F: Well purging and groundwater sampling

The well purging and subsequent sampling was done using two peristaltic pumps (see Figure A 2). The volume of water that needed to be pumped from the well during purging was calculated based on the volume of water inside the well, and multiplied by a factor of three to ensure the recharge of fresh groundwater:

$$V_{pump} = 3 * \left(\pi * \left(\frac{d_{well}}{2} \right)^2 \right) * (L_{well} - d_{gw})$$

Where the V_{pump} is the volume to be pumped, d_{well} is the inner well diameter (3.7 cm in our wells), L_{well} is the well depth (from tube top), and d_{gw} is the depth from the well top to the water level.

In some cases, recharge into the well was very slow, and in these cases, we would stop the purging when the well ran dry (i.e., before V_{pump} was reached). All wells (with water in them) were purged twice within the space of two weeks. After the second purging round (31. May 2019) and before the sampling campaign started (01. July 2019), precipitation was 68.4 mm.
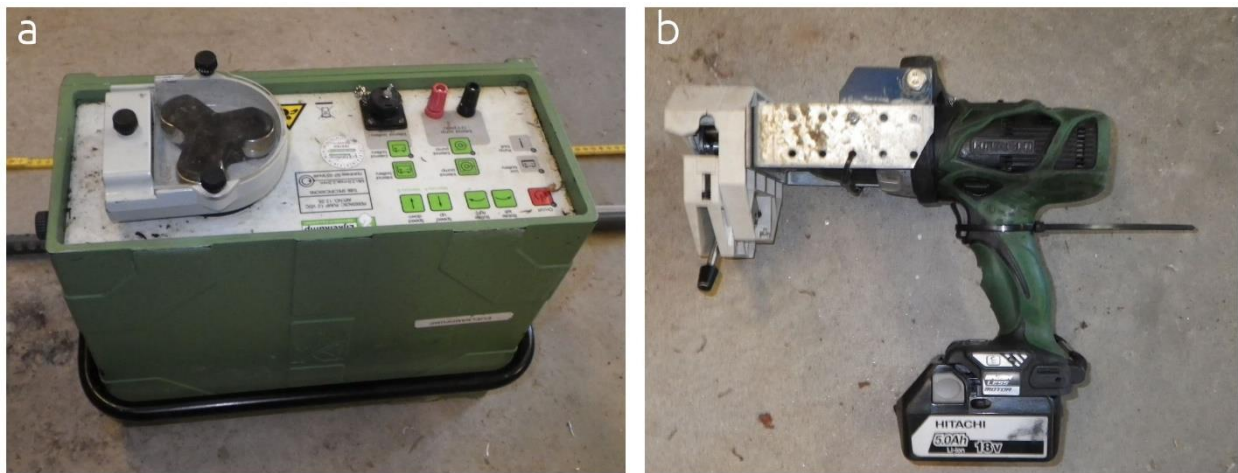
Figure A 2: Photo of peristaltic pump (a) and peristaltic pump mounted on a drill (b) used for purging the wells

For the groundwater sampling, we used a custom-made packer system (Figure A 3) that could seal off the access to water below and above the part where the sample would be taken. This allowed for sampling at discrete depths. Markers on the tube of the packer system allowed the determination of the sample depth. The packer was designed to sample up to a depth of 6 m. Since the sample opening is

located above the lowest end of the packer, a minimum water level of 40 cm inside the well was necessary to take a sample with the packer system.

Figure A 3: Photo of the custom-made straddle packer system with two inflatable parts to isolate specific depths in the wells and to pump water from specific depth (a) and the upper part and tubing system (pumping tube and two air tubes to inflate the flexibles tube parts) of the packer system (b). The yellow arrows in (a) indicate inflatable packer system parts to seal off the water above and below the selected sample depth.

Appendix G: Logger and manual water level summary

Table A 7: Summary of the recorded water level data per well and the manual measurements for each well. The summary statistics (mean, median, minimum and maximum) were only calculated over the valid data points. Note that for some wells (e.g., A45 and A50) the number of valid data points is very small because the well was dry for most of the study period or the data were flagged as censored data. *non-valid data points and manual outlier include dry well values

775

well	Logger data						Manual measurements					
	Valid data points	Non-valid data points*	mean	median	min	max	Number of measurements	Number of valid outliers*	mean	median	min	max
			water level in [m amsl]						level in [m amsl]			
A1	0	97353					0	0				
A2	97145	258	264.18	264.16	263.61	265.07	5	21	264.40	264.48	263.76	264.75
A3	90299	231	261.45	261.30	260.70	262.98	16	2	261.47	261.31	260.83	262.72
A4	96838	677	263.35	263.41	262.20	264.20	10	15	262.99	262.88	262.59	263.77
A5	67179	11803	264.93	264.87	264.40	265.65	4	13	265.09	265.08	264.88	265.33
A6	78746	234	263.47	263.43	262.04	264.29	13	4	263.51	263.52	263.02	263.88
A7	71683	8653	265.85	265.79	265.64	266.45	23	2	265.79	265.75	265.63	266.21
A8	72037	6947	262.10	261.94	261.50	263.21	7	10	262.06	262.03	261.90	262.32
A9	97084	440	261.76	261.70	260.60	263.03	16	9	261.58	261.47	261.26	262.81
A10	47317	29229	262.24	262.01	261.80	263.50	3	8	262.34	262.36	262.11	262.54
A11	97040	723	264.22	264.22	263.87	264.66	18	5	264.16	264.18	263.90	264.45
A12	97027	486	261.20	261.19	260.39	262.32	7	18	260.59	260.60	260.44	260.80
A13	70774	237	265.25	265.27	264.64	265.41	19	1	265.22	265.25	264.97	265.32
A14	2953	86887	264.37	264.37	264.23	264.67	2	0	264.26	264.26	264.19	264.33
A15	97055	416	264.21	264.22	263.18	264.48	23	3	264.23	264.24	264.08	264.32
A16	97242	187	264.11	264.14	263.51	264.34	16	10	264.14	264.14	263.99	264.25
A17	57718	32496	264.22	264.17	264.00	264.65	12	0	264.19	264.14	263.98	264.52
A18	72977	230	261.05	260.92	260.30	262.36	1	10	260.94	260.94	260.94	260.94

well	Logger data						Manual measurements					
	Valid data points	Non-valid data points *	level in [m amsl]				Number of valid measurements	Number of outliers *	level in [m amsl]			
			mean	median	min	max			mean	median	min	max
A19	78843	150	261.50	261.40	260.63	262.71	10	7	261.47	261.34	260.78	262.56
A20	86289	3549	263.56	263.60	263.02	263.74	15	1	263.53	263.55	263.16	263.65
A21	95942	1526	261.84	261.93	260.45	262.25	16	9	261.79	261.72	261.42	262.13
A22	275	78914	265.46	265.47	265.23	265.65	1	0	265.22	265.22	265.22	265.22
A23	51623	230	259.39	259.35	259.02	259.96	16	1	259.37	259.29	259.09	259.81
A24	0	71921					4	0	265.75	265.75	265.75	265.76
A25	240	114128	264.00	263.99	263.98	264.20	2	0	263.95	263.95	263.95	263.96
A26	91847	5562					0	6				
A27	97238	271	261.03	261.08	259.44	261.63	18	7	260.95	260.94	260.42	261.50
A28	79115	161	257.58	257.51	257.17	258.29	16	1	257.56	257.44	257.22	258.15
A29	60092	154	258.31	258.25	257.92	258.88	17	0	258.29	258.21	257.98	258.75
A30	66847	150	258.13	258.16	257.57	258.50	5	3	258.06	258.11	257.71	258.39
A31	75478	0	263.19	263.21	262.41	263.94	9	1	263.08	263.05	263.00	263.23
A32	75405	78	263.42	263.40	262.56	264.13	14	1	263.36	263.34	263.18	263.61
A33	264	66577	263.31	263.28	263.08	263.61	0	0				
A34	58548	1669	261.01	261.02	260.12	261.33	11	6	260.98	260.96	260.92	261.15
A35	73967	5323	261.01	261.04	260.29	261.40	13	4	261.03	261.01	260.95	261.15
A36	14769	16537	277.77	278.17	262.77	278.63	0	0				
A37	79058	235	260.73	260.79	259.85	261.27	14	3	260.76	260.78	259.98	261.01
A38	74321	153	257.16	257.15	255.57	257.35	15	0	257.14	257.12	256.95	257.26
A39	0	97756					0	0				
A40	79124	160	257.01	256.92	255.91	257.50	15	2	257.05	256.95	256.68	257.43
A41	30199	45368	261.40	261.21	260.76	262.86	1	9	260.35	260.35	260.35	260.35
A42	75399	74	261.52	261.38	261.15	263.12	0	9				

well	Logger data		level in [m amsl]				Manual measurements		level in [m amsl]			
	Valid data points	Non-valid data points *	mean	median	min	max	Number of valid measurements	Number of outliers *	mean	median	min	max
A43	79132	154	257.12	257.06	256.20	257.85	11	6	257.16	257.05	256.96	257.64
A44	65520	19891	259.35	259.04	258.56	261.67	8	10	259.12	258.86	258.46	260.42
A45	16346	71051	260.87	261.01	259.99	261.29	2	10	260.56	260.56	259.98	261.14
A46	79061	228	257.07	257.03	256.55	257.81	11	5	256.92	256.75	256.75	257.58
A47	79068	227	256.68	256.67	255.61	257.02	2	15	256.66	256.66	256.59	256.74
A48	23935	99650	260.96	261.03	259.68	261.89	4	9	261.18	261.22	260.53	261.76
A49	2960	94487	258.55	258.55	258.46	258.64	0	0				
A50	23010	48967	261.07	260.89	260.89	262.23	0	5				
A51	32573	64715	257.09	257.08	256.38	258.04	4	4	256.58	256.56	256.45	256.76
A53	68316	7243	257.08	256.76	256.42	259.28	9	1	256.83	256.83	256.47	258.62
A54	56619	18909	257.37	256.98	256.58	259.23	8	6	257.47	257.33	256.50	258.82
B1	75616	6502	263.88	263.81	263.04	265.20	13	2	263.79	263.83	263.47	264.15
B2	66356	5438	261.87	262.07	260.92	262.30	0	11				
B3	71507	286	261.53	261.43	261.01	262.43	11	0	261.51	261.47	261.03	261.98
B4	75555	6570	259.39	259.27	258.65	260.56	13	2	259.28	259.28	258.68	260.17
B5	65675	16455	258.45	258.28	258.02	259.66	7	8	258.18	258.15	257.92	258.38
B6	56558	23909	258.77	258.59	258.41	259.95	4	11	258.50	258.40	258.35	258.84
B7	63063	6419	259.25	259.14	258.44	260.44	3	0	258.79	258.83	258.62	258.92
B8	68540	156	259.53	259.43	258.72	260.78	9	0	259.25	259.35	258.99	259.48
B9	75628	76	257.76	257.61	257.10	259.13	12	3	257.70	257.61	257.13	258.58
B10	12001	63102	258.80	258.78	258.19	259.40	1	8	257.57	257.57	257.57	257.57
B11	75621	6595	259.39	259.35	258.71	260.58	15	0	259.33	259.35	258.89	259.72
B12	74599	7516	257.51	257.47	257.00	258.45	5	10	257.32	257.47	257.00	257.62
B13	75622	6496	257.26	257.25	256.78	258.35	4	11	257.34	257.34	257.18	257.49

well	Logger data						Manual measurements					
	Valid data points	Non-valid data points *	level in [m amsl]				Number of valid measurements	Number of outliers *	level in [m amsl]			
			mean	median	min	max			mean	median	min	max
B14	68391	7308	257.24	257.25	255.94	257.54	0	15				
B15	23385	52314	256.40	256.26	255.97	257.28	0	15				
B16	75618	80	256.85	256.83	255.83	257.30	10	5	256.70	256.78	256.30	256.98
B17	67719	7982	255.54	255.38	255.14	256.68	8	7	255.45	255.37	255.18	255.90
B18	75624	78	254.71	254.67	254.11	255.51	14	1	254.59	254.62	254.13	255.06
B19	69087	6614	253.68	253.53	253.23	254.28	11	4	253.60	253.49	253.15	254.18
B20	40737	816	253.53	253.41	252.85	254.50	13	0	253.36	253.37	252.82	254.02